REVIEW ARTICLE



Human brain clearance imaging: Pathways taken by magnetic resonance imaging contrast agents after administration in cerebrospinal fluid and blood

Matthias J. P. van Osch ¹ Anders Wåhlin ^{2,3,4} Paul Scheyhing ^{5,6}
Ingrid Mossige ^{7,8} Lydiane Hirschler ¹ Anders Eklund ^{2,4}
Klara Mogensen ² Ryszard Gomolka ⁹ Alexander Radbruch ^{5,6}
Sara Qvarlander ² Andreas Decker ⁶ Maiken Nedergaard ^{9,10}
Yuki Mori ⁹ Per Kristian Eide ^{11,12} Katerina Deike ^{5,6} Geir Ringstad ^{13,14}

¹C. J. Gorter MRI Center, Department of Radiology, Leiden University Medical Center (LUMC), Leiden, The Netherlands

Correspondence

Matthias J. P. van Osch, C. J. Gorter MRI Center, Department of Radiology, Leiden University Medical Center (LUMC), Leiden, The Netherlands.

Email: m.j.p.van_osch@lumc.nl

Funding information

This review was funded by the HCBI project. The HCBI-project ("Human brain clearance imaging: a window on physiological disturbances in the prediagnostic phase of neurodegenerative diseases") is an EU Joint

Abstract

Over the last decade, it has become evident that cerebrospinal fluid (CSF) plays a pivotal role in brain solute clearance through perivascular pathways and interactions between the brain and meningeal lymphatic vessels. Whereas most of this fundamental knowledge was gained from rodent models, human brain clearance imaging has provided important insights into the human system and highlighted the existence of important interspecies differences. Current gold standard techniques for human brain clearance imaging involve the injection of gadolinium-based contrast agents and

Abbreviations: AD, Alzheimer's disease; AIF, arterial input function; BBB, blood-brain barrier; BG, basal ganglia; CE, contrast-enhanced; CNS, central nervous system; CSF, cerebrospinal fluid; DCE, dynamic contrast-enhanced; DSC, dynamic susceptibility contrast; ESUR, European Society of Urogenital Radiology; Gd, gadolinium; glymphatic, glial-lymphatic; HBCI, human brain clearance imaging; iNPH, idiopathic normal-pressure hydrocephalus; IPAD, intramural periarterial drainage; JPND, EU Joint Programme – Neurodegenerative Disease Research; MRI, magnetic resonance imaging; MS, multiple sclerosis; PVS, perivascular spaces; SAS, subarachnoid space; VCI, vascular cognitive impairment; WM, white matter.

This is an open access article under the terms of the Creative Commons Attribution License, which permits use, distribution and reproduction in any medium, provided the original work is properly cited.

© 2024 The Authors. NMR in Biomedicine published by John Wiley & Sons Ltd.

 $^{^2}$ Department of Radiation Sciences, Radiation Physics, Biomedical Engineering, Umeå University, Umeå, Sweden

³Department of Applied Physics and Electronics, Umeå University, Umeå, Sweden

⁴Umeå Center for Functional Brain Imaging, Umeå University, Umeå, Sweden

⁵Department of Neuroradiology, University Medical Center Bonn, Rheinische Friedrich-Wilhelms-Universität Bonn, Bonn, Germany

⁶German Center for Neurodegenerative Diseases (DZNE), Bonn, Germany

⁷Division of Radiology and Nuclear Medicine, Department of Physics and Computational Radiology, Oslo University Hospital, Oslo, Norway

⁸Institute of Clinical Medicine, The Faculty of Medicine, University of Oslo, Oslo, Norway

⁹Center for Translational Neuromedicine, University of Copenhagen, Copenhagen, Denmark

¹⁰Center for Translational Neuromedicine, University of Rochester Medical Center, Rochester, New York, USA

¹¹Department of Neurosurgery, Oslo University Hospital-Rikshospitalet, Oslo, Norway

¹²KG Jebsen Centre for Brain Fluid Research, Institute of Clinical Medicine, Faculty of Medicine, University of Oslo, Oslo, Norway

¹³Department of Radiology, Oslo University Hospital-Rikshospitalet, Oslo, Norway

¹⁴Department of Geriatrics and Internal Medicine, Sorlandet Hospital, Arendal, Norway

Programme-Neurodegenerative Disease
Research (JPND) project. The project has
received funding from the European Union's
Horizon 2020 Research and Innovation
Programme under grant agreement
No. 825664. Additional funding was received
by Alzheimer Netherland (MJPvO, LH),
Netherlands Organisation for Scientific
Research (NWO) (MJPvO, project M20-238),
Swedish Research Council (AW, 2022-04263),
the Swedish Foundation for Strategic Research
(AE), and The Research Council of Norway
(RCN) (GAR, project 333956).

monitoring their distribution and clearance over a period from a few hours up to 2 days. With both intrathecal and intravenous injections being used, which each have their own specific routes of distribution and thus clearance of contrast agent, a clear understanding of the kinetics associated with both approaches, and especially the differences between them, is needed to properly interpret the results. Because it is known that intrathecally injected contrast agent reaches the blood, albeit in small concentrations, and that similarly some of the intravenously injected agent can be detected in CSF, both pathways are connected and will, in theory, reach the same compartments. However, because of clear differences in relative enhancement patterns, both injection approaches will result in varying sensitivities for assessment of different subparts of the brain clearance system. In this opinion review article, the "EU Joint Programme - Neurodegenerative Disease Research (JPND)" consortium on human brain clearance imaging provides an overview of contrast agent pharmacokinetics in vivo following intrathecal and intravenous injections and what typical concentrations and concentration-time curves should be expected. This can be the basis for optimizing and interpreting contrast-enhanced MRI for brain clearance imaging. Furthermore, this can shed light on how molecules may exchange between blood, brain, and CSF.

KEYWORDS

brain clearance, cerebrospinal fluid, glymphatics, intrathecal injection, intravenous injection

1 | INTRODUCTION

Over the past decade, neuroscience has gone through a paradigm shift in how to regard the purpose of cerebrospinal fluid (CSF) and its circulation. Tenacious dogmas about where CSF is produced and resorbed are currently up for revision, and the pivotal role of CSF in perivascular brain solute clearance and interactions between the brain and meningeal lymphatic vessels have sparked the research field of human brain clearance imaging. Important hallmarks of neurodegenerative diseases, such as cerebral amyloid angiopathy, Alzheimer's disease (AD), and Parkinson's disease, involve depositions of proteins in the brain tissue or the cerebral vasculature, with amyloid- β , phosphorylated tau, and α -synuclein being the most important examples.^{2,3} Impaired brain clearance could therefore be an important underlying process starting, accompanying, or aggravating these debilitating diseases. The dogma on the absence of a lymphatic-like system in the brain was slowly debunked around the 2010s with important research into the glial-lymphatic (glymphatic) system, intramural periarterial drainage (IPAD) pathway, and dural lymphatic vasculature.4-11 However, it has yet not been established to what extent solute drainage along or within vessel walls adds to the clearance of solutes over the blood-brain barrier (BBB) and via microglia. 12 These new insights, in combination with the still existing knowledge gaps, have led to a steep increase of interest in the development and application of imaging techniques to monitor this system. ¹³ Magnetic resonance imaging (MRI) is the first candidate for human brain clearance imaging, because of its diverse capabilities, safety profile, and its dominant role in the imaging of neurodegenerative diseases. Among different MRI techniques pursued for brain clearance imaging, contrast-enhanced (CE) techniques allow tracking of an exogenous tracer to resemble the movement of endogenous solutes in vivo, and not just the solvent (water). There are currently two different approaches to CE-MRI for human brain clearance imaging: administration of contrast agent into the blood pool (intravenous), 14,15 and directly into the CSF compartment (intrathecal). ¹⁶ As intrathecally injected contrast agents will also end up in the blood pool ¹⁷ and intravenously injected contrast agent will reach CSF, 18 for example, in the subarachnoid space (SAS), both systems are connected and both approaches will finally reach the same compartments. However, the relative contrast agent concentrations, as well as the temporal enhancement patterns, will be different. Thus, the specificity of the signal enhancement within the perivascular pathways will be different because of the differences in contrast agent concentrations in adjacent compartments (e.g., perivascular and intravascular compartments). Because of bidirectional contrast agent exchange between the blood and CSF compartments, both intravenous and intrathecal administration provide complementary information about the brain clearance pathways and their functionality, however, with varying sensitivities for the assessment of different subsystems.

Here, we provide an overview on observational research of contrast agent pharmacokinetics in vivo following intrathecal and intravenous injections. We also discuss which typical concentrations and concentration–time curves should be expected. This can serve as the basis for optimizing and interpreting CE MRI for brain clearance imaging. Furthermore, it can shed light on how molecules may exchange between blood and

CSF. We refer to the supporting information for tables with a bibliographic overview of literature published on the two injection approaches (Tables S1 and S2).

2 | BASIC PROPERTIES OF THE BLOOD AND CSF CIRCULATIONS

To establish an approach to investigate the relations between glymphatic pathways, brain parenchyma, and the circulations of blood and CSF, we need to clarify some features of these interacting compartments. The total volume of blood of an adult is approximately 7% of the body weight, or 5 L. Of this, 15% of the cardiac output perfuses the brain, even although the brain accounts for only 2% of the body volume, showing its high metabolic demand. The brain is a very well perfused organ with a cerebral blood flow in the gray matter of typically 60 mL/100 g/min and 25 mL/100 g/min in the white matter (WM). This is equivalent to 750 mL of blood entering the brain in young adults each minute, which gradually decreases to 500 mL/min in 80-year-old subjects.¹⁹

It is generally assumed that a young healthy subject has approximately 150 mL of CSF, of which 125 mL is located in the spinal and cranial SASs and 25 mL is within the cerebral ventricles.^{20,21} MRI data provided much higher values of 331 mL for total CSF, of which 74 mL was located in the spinal canal,²² and the differences vary significantly between subjects, but for the remainder of this article we will use the textbook numbers, while accepting that these numbers need to be validated. The total secretion of CSF is commonly estimated to between 400 and 600 mL per day.²³ CSF consists for the largest part of water (99%), but importantly it also contains electrolytes, proteins, and neurotransmitters, with concentrations very similar to those in plasma,²⁴ whereas glucose levels are one-half of those in serum.²⁵ The exchange of these substances between blood and CSF is supported by active transport mechanisms across the blood–CSF barrier within the choroid plexus, whereas water exchange between CSF and blood is more widespread throughout the brain.^{26,27} Finally, absorption of CSF has traditionally been assumed to mainly occur via the arachnoid granulations, while other pathways, including the dural lymphatic vessels, optic and other cranial nerves, and from the spinal canal, have also been proposed.²⁰

3 | PROPERTIES OF MRI CONTRAST AGENTS AS CLEARANCE TRACER

Macrocyclic gadolinium (Gd)-based MRI contrast agents are hydrophilic, small, and inert complexes, which makes them potential exogenous CSF clearance tracers. For example, gadobutrol has a molecular weight of 604 Da and an estimated hydraulic diameter of less than 2 nm. Therefore, once intrathecally injected or penetrating from blood into the CSF, it is expected to enter perivascular spaces (PVS) and from there the brain interstitium. The drivers and molecular entry points for this perivascular-interstitial fluid exchange are not finally resolved. According to the glymphatic theory, gadobutrol is proposed to cross from the perivascular space into the brain interstitial space via gaps between the astrocytic end feet, which constitute the peripheral PVS boundary. Compared with many of the endogenous brain solutes that are cleared from the brain along perivascular pathways, gadobutrol is much smaller and therefore more susceptible to diffusional forces.

4 | INTRATHECAL INJECTION

The first observations with intrathecal contrast agent injections started from imaging in patients with suspected intracranial hypotension due to spontaneous CSF leakage.²⁹ Previous rodent studies,³⁰ and the observation that the contrast agent distributes throughout the spinal CSF and further into the brain, before its subsequent clearance, led to the breakthrough concept of using intrathecal contrast agent as CSF tracer to characterize brain clearance and the CSF circulation.³¹ Spread of intrathecally injected contrast agent from the spinal canal into the intracranial compartment is fast; in a study of 100 subjects, spinal transit time after lumbar injection was on average 20 ± 23 min, with a median of 13 min; and a range of 6–150 min.³² The methodology allows for studies of long-term CSF flow patterns, brain tissue enrichment, and subsequently clearance. Macrocyclic Gd-based MRI contrast agents are suitable for tracking extravascular molecular motions in brain when administered intrathecally, as they are hydrophilic and inert molecules of small size, and are expected to leak into brain blood vessels to a very minor extent when the BBB is intact. Later studies in numerous subjects have shed light on patterns of tracer enrichment and its clearance rate from the brain, as well as pharmacokinetics concerning clearance from CSF to the blood pool. 17,33 Importantly, it was shown that clearance of contrast agent from the brain was delayed when the subjects were sleep-deprived, confirming early observations in rodents that brain clearance is enhanced during deep sleep, albeit pointing towards a smaller effect in humans compared with mice.^{6,34} This also confirms that intrathecal injections are able to capture important functional properties of the brain clearance system. Although the application of intrathecal injections to study brain clearance has mainly been developed and applied in a single site (Oslo, Norway), other sites are now also performing such studies.^{35–37} Figure 1 provides a schematic overview of how the contrast agent is distributed and subsequently cleared. In the following sections, we discuss these processes in greater detail.

1099142, 2024, 9, Downloaded from https://analyticalsciencejournals.onlinelibrary.wiley.com/do/10.1002/nbm.5.159 by Joleen McImis - Deutsches Zentrum Für Neurodog, Wiley Online Library on [08/08/2024]. See the Terms and Conditions (https://onlinelibrary.wiley.com/erems-

and-conditions) on Wiley Online Library for rules

of use; OA articles are governed by the applicable Creative Commons License

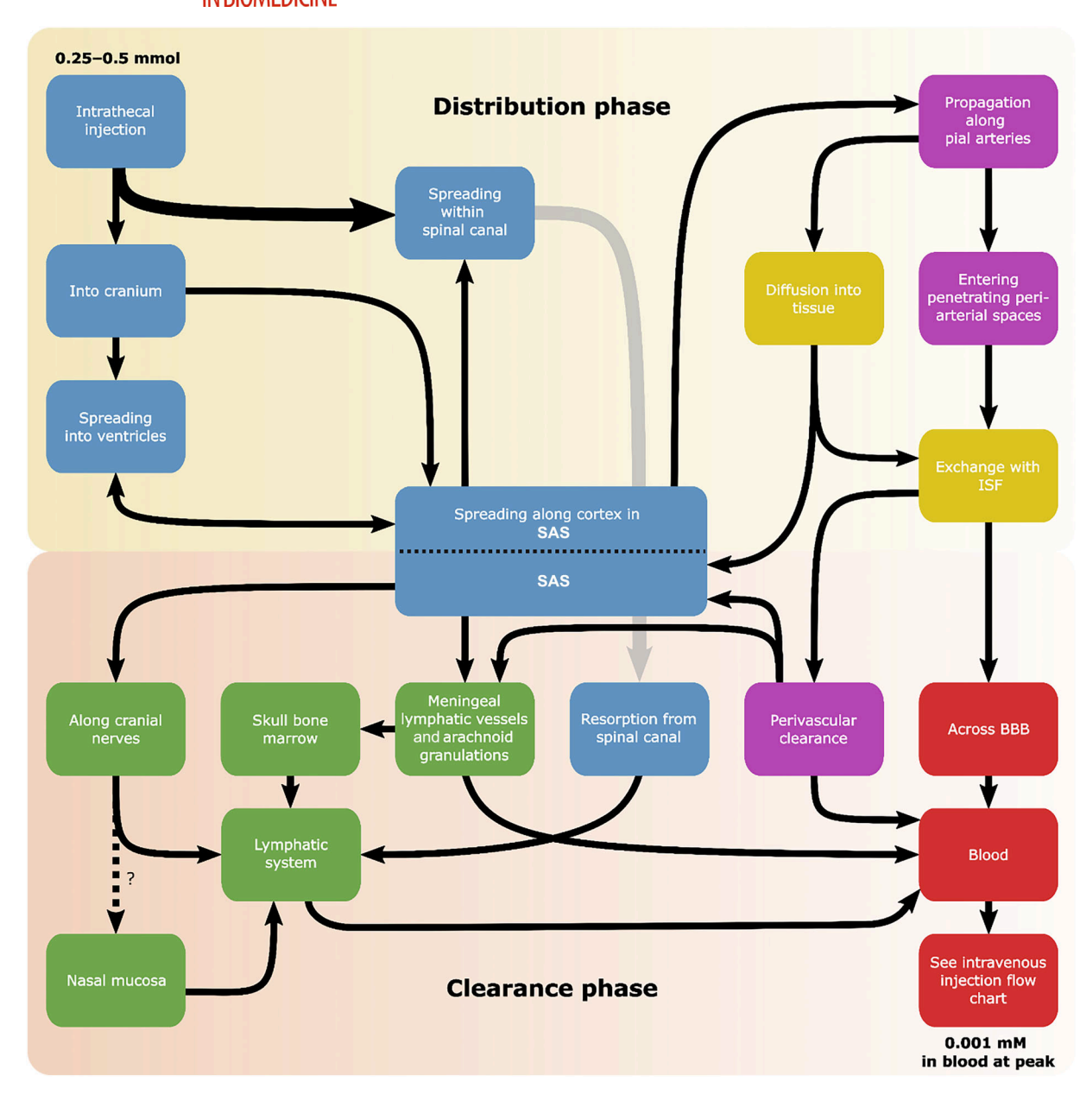


FIGURE 1 A schematic overview of pathways taken by contrast agent after an intrathecal injection. Note that contrast agent will be taken up by blood, which can be seen as entering the same pathway as via intravenous injections. Blue boxes indicate large CSF spaces, green the lymphatic system, yellow interstitial spaces, purple spaces around vessels, and red the blood compartments. Possible compartmentalization within the SAS is indicated by a dashed line. Note that in the bottom-right corner a crossover is made to the flowchart of intravenous injections, because the contrast agent has reached the blood compartment. BBB, blood-brain barrier; CSF, cerebrospinal fluid; ISF, interstitial fluid; SAS, subarachnoid space.

4.1 | Intrathecal injection protocol

Intrathecal injections are performed at lumbar level and mainly with doses of 0.50 and 0.25 mmol of gadobutrol (Gadovist; Bayer Pharma AG, Berlin, Germany), a 1.0 M contrast agent. Smaller doses (0.10 mmol) were found to be too low for adequate imaging at 1.5 T.³⁸ Safety studies have shown that injections of 0.50 and 0.25 mL of gadobutrol are in general well tolerated.^{32,39,40} Typically, intrathecal injection is performed by mixing gadobutrol with saline in a 1-mL syringe to prevent inadvertent injection of larger doses that may cause neurotoxicity, as serious side effects have been reported in doses of 2 mmol and higher only.⁴¹ In the human CSF compartment, a slow injection of 1 mL of fluid at the lumbar level is expected to have no significant influence on intracranial pressure, nor should a potentially subtle CSF leak postpuncture. The typical injection duration is 10–20 s. We refer to the Discussion section for a more elaborate overview on the safety of intrathecal injections. Typically, the

patient is restricted to remain in bed and in the supine position for at least 3-4 h after injection, both for standardization of the procedure and to prevent postpuncture headache. Before intrathecal injection, acquisition of a 3D T_1 -weighted scan or T_1 map of the head is performed to establish a baseline for subsequent contrast enhancement of the CSF spaces and brain tissue. Because of image rescaling between scans at different timepoints, readout of grayscale signal units from consecutive T_1 -weighted images need to be normalized against a reference tissue; typically, intraorbital fat has been used. However, T_1 -weighted images render semiquantitative measures only, making it important that more studies should adopt T_1 mapping to estimate the absolute concentration-time curves for gadobutrol in brain.

4.2 | Distribution of intrathecal contrast agent within CSF spaces

After intrathecal injection of gadobutrol at the lumbar level, the tracer propagates upwards within the spinal canal and was found, on average, to reach the SAS at the level of the foramen magnum in 22 ± 34 min in supine patients, thus with large interindividual differences. In some cases the transit time was only 5 min. In addition to dispersion in CSF, distribution within the spinal canal is thought to be especially driven by intrathoracic pressure changes that occur over the respiratory cycle. Furthermore, a previous phase-contrast MRI study found cranially directed net CSF flow at the level of the craniocervical junction in supine patients. Importantly, an extensive spinal resorption of the tracer occurs and approximately only one-quarter of the injected tracer reaches the brain. In 17,45

Using a "back-of-the-envelope" calculation to shed some light on the influence on the MRI signal, we can calculate the resulting concentrations of contrast agent from the applied doses (0.50 and 0.25 mmol, respectively) and the estimated total volume of CSF of 150 mL. This would result in concentrations of 3.3 and 1.7 mM, respectively, when the contrast agent is perfectly mixed within the total CSF volume and before any resorption from CSF occurs. When assuming a relaxivity of 3.9 s⁻¹ mM⁻¹ and a baseline T_1 of CSF of 4300 ms at 3 T, this would result in a T_1 of 76 and 145 ms, respectively, at these equilibrium concentrations. Such short T_1 s can provide more than enough MR-signal enhancement to allow monitoring of the pathways taken by the contrast agent, as is also evident from in vivo imaging (Figure 2). Quantitative measurements of contrast agent concentration in the CSF after intrathecal injection showed lower concentrations than the abovementioned perfect theoretical

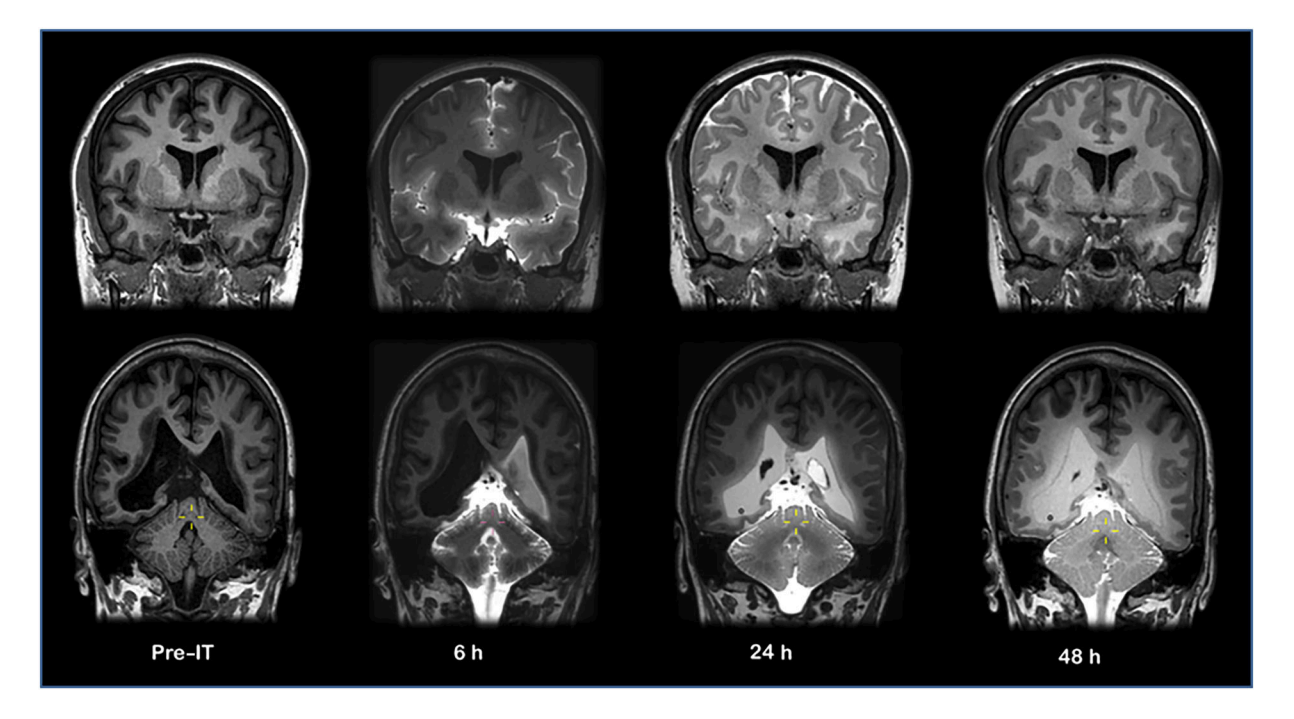


FIGURE 2 Various CSF tracer enhancement patterns in subarachnoid and ventricular spaces. Coronal T₁-weighted images obtained at consecutive timepoints from preintrathecal injection of 0.5 mmol of gadobutrol (left column) through 6 and 24 h (middle columns) to 48 h after injection (right column). Window and level settings of each image have been adjusted manually to optimize visualization of tracer enhancement in both CSF and parenchyma. Upper row: patient under work-up of CSF disorder, but where no treatable condition was diagnosed (reference patient). The CSF tracer distributes around the entire cerebral hemispheres and peaks in intensity at 24 h. Lower row: patient with communicating hydrocephalus. A substantial and persisting ventricular reflux of CSF tracer is observed; at 24 and 48 h there is also a periventricular signal increase as a sign of transependymal efflux. However, enrichment around the cerebral hemispheres is very sparse and not seen at the upper convexities at any timepoint. CSF, cerebrospinal fluid; IT, intrathecal injection.

0991492, 2024, 9, Downloaded from https://analyticalscie

concentration; that is, in a quantitative study, Watts et al. reported, albeit only in a single subject, concentrations of up to 0.6 mM in the CSF of the insula after intrathecal injection of 0.50 mL of 1 mM gadobutrol.³⁵ The concentration measured by Watts et al. corresponds to a T_1 of 390 ms. This difference can be explained by resorption from the spinal canal and at cranial nerve outlets at the base of the skull before the tracer reaches the intracranial space, as well as imperfect mixing.

From the cisterna magna, the tracer quickly enriches the subarachnoid cisterns at the base of the skull, after which distribution in the antegrade direction along the large artery trunks within the major cerebral fissures occurs. The possible influence of layers within the SAS that could compartmentalize the spreading of contrast agent within this space is still an open research question.⁴⁸ We indicate possible compartmentalization within the SAS by a dashed line in Figure 1. A perivascular distribution pattern within the SAS, and with a delay of propagation in idiopathic normal-pressure hydrocephalus (iNPH), was previously shown (see fig. 3 in Ringstad et al.³¹). At MRI scans obtained after 24 h, the tracer has typically enhanced diffusely around the entire brain.³¹ Still, major differences in the enhancement of CSF spaces have been observed, even at late scans (as exemplified in Figure 2). In iNPH, lack of enhancement outside the upper brain convexities and also in single sulci ("trapped sulci") is typically accompanied by an early and strong ventricular tracer reflux that persists for as long as there is tracer left at the brain surface.⁴⁹ In patients with spontaneous intracranial hypotension due to CSF leakage, tracer enhancement is also typically very sparse around the upper brain convexities (Figure 3). Lack of any enhancement through 48 h at the surface of some brain regions raises the question of to what extent CSF-interstitial fluid (ISF) exchange in those regions contributes to brain clearance, and from where CSF in those regions is originating, while obviously not from the ventricles.

4.3 | Distribution of intrathecal contrast agent in the brain

Gadobutrol has been shown to enrich all subregions of the brain from the cortical surface centripetally; however, this mostly happens in the cortex, and to some extent in the subcortical WM, mainly in the immediate vicinity of the cortex¹⁶ (Figure 4). Tracer enhancement in deep WM is very limited, suggesting CSF-ISF exchange has a less important role here, and that analyses of deep WM diffusional properties⁵⁰ or enlarged PVS in WM⁵¹ may be of limited value for assessment of brain cortical (glymphatic) clearance mediated by CSF. However, it needs to be mentioned that currently little is known regarding this topic, and that this statement is solely based on observations from intrathecal injections. Presence of the tracer in CSF spaces adjacent to brain tissue is highly associated with local tissue uptake.¹⁶ The first and most vivid enhancement is in areas of the cerebral cortex adjacent to the large artery trunks, where CSF enhancement occurs first and is most pronounced. Interestingly, the entorhinal cortex, where neurodegeneration typically starts, is also one of the regions with the highest degree of

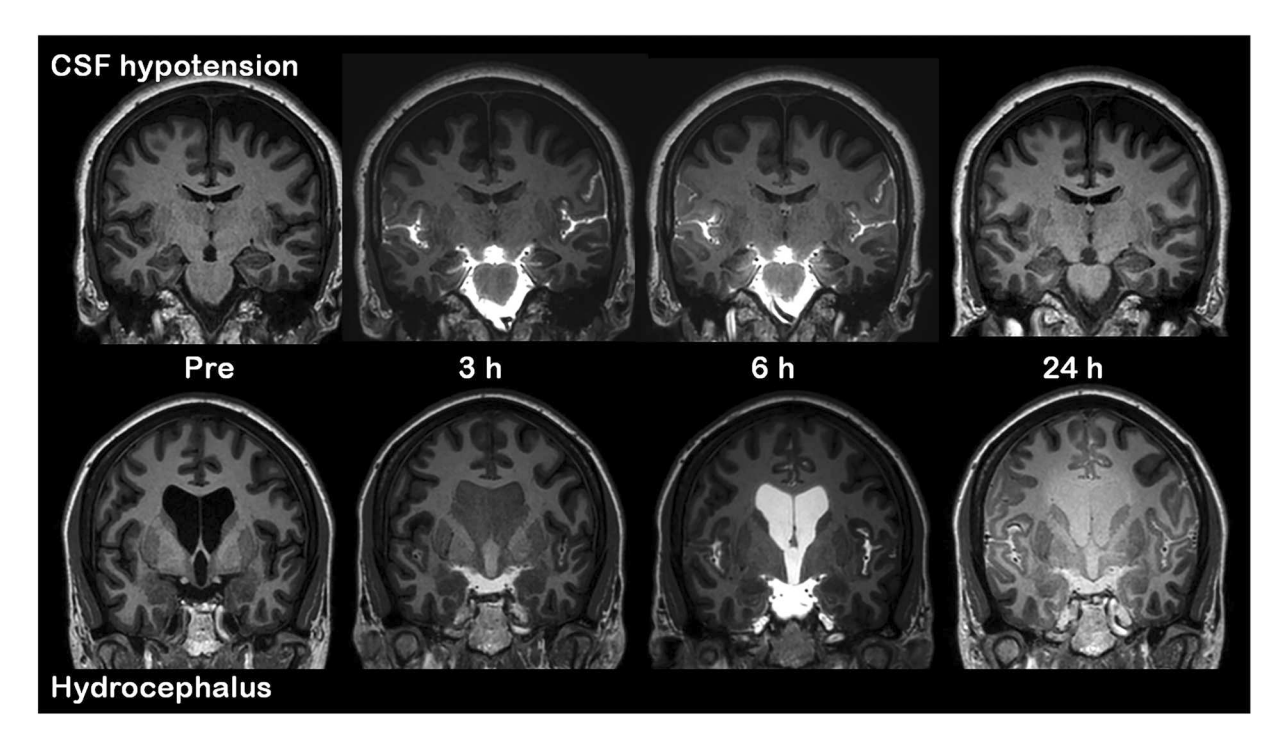


FIGURE 3 Two patient examples, where very sparse enhancement around the upper brain convexities can be observed. CSF, cerebrospinal fluid.

FIGURE 4 CSF tracer enhancement in the brain tissue. Consecutive T_1 -weighted images obtained before and through 1–24 h after contrast injection, shown in three orthogonal planes from a patient under work-up of CSF circulation disorder (no treatable condition was diagnosed, "reference patient"). Upper row: midsagittal sections; middle row: midcoronal sections, and lower row: midaxial sections. Percentage increase of normalized T_1 signal units in the brain tissue is given on a color scale, indicating enhancement of MRI contrast agent (gadobutrol) when utilized as CSF tracer. Nonbrain tissue was removed using a hybrid watershed/surface deformation procedure, as described in Ringstad et al. (Illustration: Vegard Vinje, PhD, Simula Research Laboratory, Oslo, Norway). CSF, cerebrospinal fluid.

CSF-ISF exchange in humans.⁵² CSF tracer enhancement patterns in the brain also correspond (to some extent) with propagation patterns of some neurodegenerative diseases.⁵³

Being a small molecule, gadobutrol propagation in brain tissue is expected to be largely governed by diffusional forces, ⁵⁴ although the image resolution of MRI does not allow for directly depicting whether there is a component of advective flow within brain tissue. However, computational modeling that was based on data from intrathecal enhanced MRI has shown that diffusion alone does not explain the tracer movements in brain parenchyma. ⁵⁴ Rather, the molecular movements in brain tissue must be driven by either substantially enhanced (3.5x) extracellular diffusion in combination with local clearance, or by extracellular diffusion augmented by advection with brain-wide average flow speeds of the order of 1–9 μ m/min. ⁴⁵ It was further shown that after approximately 6 h, nearly one-quarter (23% ± 10%, 0.116 ± 0.051 mmol) of the 0.50-mmol tracer injection had entered the brain. The maximal amount of tracer (25% ± 10%, 0.125 ± 0.050 mmol) is found within the brain after 24 h, while 14% ± 7% (0.068 ± 0.034 mmol) remains in brain tissue after 48 h. The main fraction of tracer enrichment in the brain reaches the cerebral cortex, while less than 0.06 mmol also enters the subcortical WM. ⁴⁵ The observed differences in how fast the contrast agent is cleared from the brain among study participants might very well be attributed to interindividual differences in CSF clearance, because levels of tracer in CSF and brain are highly associated. ⁵²

4.4 | Clearance of intrathecally injected contrast agent

After administration of gadobutrol tracer into the CSF at lumbar level, early clearance is probably dominated by resorption from the spinal compartment and at the skull base. The concentration of gadobutrol in blood peaks approximately 6 h after intrathecal injection in reference subjects and reaches a maximum concentration of approximately 1.4 μ M.^{17,33} At this timepoint, enrichment around upper brain convexities is very sparse, demonstrating that CSF clearance from the spinal canal and possibly via cranial nerve outlets at the base of the skull can be a major determinant for total CSF clearance capacity. Interestingly, the presence of contrast agent in blood can now be seen as a crossover to intravenous contrast agent injections. However, it should be emphasized that the concentration of gadobutrol in blood after intrathecal injection (\approx after 5–6 h) is approximately a factor of 3000 smaller than those observed after an intravenous injection.¹⁷

In patients with a complete absence of enhancement at the upper brain convexities at all observed timepoints throughout 48 h, clearance of tracer still occurs, and typically at a normal pace, further suggesting that, overall, CSF resorption via arachnoid granulations along the superior

0991492, 2024, 9, Downloaded from https://analyticalscier

journals.onlinelibrary.wiley.com/doi/10.1002/nbm.5159 by Joleen

McInnis - Deutsches Zentrum Für Neurodeg, Wiley Online Library on [08/08/2024]. See the Terms and Conditions (https://onlinelibrary.wiley.

of use; OA articles are governed by the applicable Creative Commons

sagittal sinus has a limited role in CSF clearance. In line with this, there was no correlation between time to peak concentration of gadobutrol in blood and peak tracer enrichment in parasagittal dura.⁵⁵ Nevertheless, CSF efflux to parasagittal dura has been visualized, rendering brain-immune cross-talk in parasagittal dural stroma⁵⁶ and efflux to peripheral lymphatic vessels, which has been demonstrated previously in rodent studies.⁵⁷⁻⁵⁹ The temporal enhancement pattern in parasagittal dura follows a similar profile to that observed in CSF, albeit with a slightly lower amplitude.⁶⁰ Maximum enhancement is observed 24 h after intrathecal injections. A high association between tracer level in parasagittal dura and adjacent CSF speaks in favor of direct efflux to parasagittal dura, possibly directly to intradural arachnoid granulations,⁶¹ or through endothelial lined channels from the SAS to dura.⁶² CSF efflux has also been shown to occur in skull bone marrow at the upper cranial vault,⁶³ enabling neuroimmune cross-talk between the brain and the central immune system.⁶³ A similar efflux pathway to vertebral bone marrow is likely in humans, considering early reports from animal studies, showing that myeloid cells from adjacent bone marrow can infiltrate the spinal dura directly through distinct channels.⁶⁴ CSF efflux along cranial nerve outlets at the skull base has been confirmed visually with MRI, but not quantified,⁶⁰ while efflux to nasal mucosa, which is a major efflux pathway in animals, was shown to be of minor importance in humans.⁶⁵ The latter finding adds to several species' differences between humans and rodents, including differences in gyration of the cerebral surface and vastly different time scales of tracer enhancement and clearance, demonstrating that human translational studies are required.

A previous finding of synchronous peak tracer enhancement at 24 h in brain tissue and deep cervical lymph nodes provided some indication of a direct link between the brain and the lymphatic system.⁶⁶ However, later studies have consistently shown a strong association between the level of tracer in SAS and adjacent brain tissue, clearly suggesting that brain clearance is highly dependent on CSF clearance,⁵² which is in accordance with the sink hypothesis⁶⁷ or the mixing model.^{68,69} It is therefore of high significance that CSF-to-blood clearance was shown to differ substantially at both disease group level and at an individual level within groups.³³ Population pharmacokinetic modeling of CSF clearance demonstrated that even very low levels of the tracer (0.10 mmol) could theoretically be utilized, suggesting that intrathecal administration of a very low amount of gadobutrol can be applied as a clinical test to assess CSF-to-blood clearance, and thus to provide a surrogate marker of the brain and meningeal lymphatic clearance. Furthermore, a later study showed that both brain (glymphatic) clearance and CSF (lymphatic) clearance was associated with diurnal fluctuations of neurodegeneration biomarkers in blood.⁷⁰

Evidence of a continuous perivascular clearance pathway from the brain into meningeal lymphatic pathways is sparse, but has been suggested in one study utilizing intravenous contrast agent, where enhancement along cortical veins was demonstrated in a case series after experimental opening of the BBB.⁷¹ However, the phenomenon was only depicted in a proportion of study subjects, and was only seen at early timepoints when levels of circulating intravenous contrast agent were high, not after 24 h. The possibility of direct perivenous leakage from blood after the accidental impact of ultrasound waves in the perimeter of the target area was not discussed. Image resolution with MRI is too low to depict details at this level, but, to date, observations with intrathecal enhanced MRI cannot rule out important contributions by diffusion and perivascular transport back into CSF, or by leakage to blood across the BBB. It should be noted that preclinical studies have shown that intraparenchymal injected fluorescent tracers always accumulate along the large veins and drain along the venous sinus in mice and rats, and that tracers injected into CSF will enter the brain parenchyma along the PVS surrounding penetrating arteries, but over time accumulate along veins. 2

Finally, at 4 weeks postinjection, there have been no depositions of contrast agent in the brain identified using MRI, either semiquantitatively.¹⁶ or quantitatively.⁷³

5 | INTRAVENOUS APPROACHES FOR BRAIN CLEARANCE IMAGING

Intravenous injections also cause contrast uptake in the extravascular compartments of the central nervous system (CNS), thereby potentially allowing the characterization and quantification of brain clearance and its pathways. Because intravascular injections are considered much less invasive than intrathecal injections, they might become a minimally invasive alternative, enabling broader research applications, and could potentially be introduced in clinical practice. Akin to intrathecal injection, intravenous injections have also been used to demonstrate the dependence of the clearance function on sleep. Tation of similar to the intrathecal approach, brain clearance function could theoretically (or at least conceptually) be inferred from the rate of decrease in postcontrast brain tissue MRI enhancement, either assessed qualitatively on post-Gd T₁ images or by quantitative T₁-mapping, while especially heavily T2-weighted 3D fluid-attenuated inversion recovery (FLAIR) and 3D-real inversion recovery sequences are able to visualize low contrast agent concentrations in the CSF spaces. Interpretation of the clearance function from the measured signal evolution following such intravenous injections might, however, be challenging, as the contrast leakage from the intravascular compartments into the CNS can occur via multiple routes characterized by different concentration-time dynamics, and because the high blood concentrations can overshadow more subtle extravascular signals.

The possible routes can be broadly categorized as (i) BBB-dependent diffuse brain-wide leakage across the capillary wall into the ISF, as well as (ii) leakages across other interfaces with naturally weak barrier properties (e.g., the choroid plexus, pial vessels, blood-ocular barrier) (Figure 5). Figure 6 shows example images of enhancement patterns 3 h postintravenous injection.

10991492, 2024, 9, Downloaded from https://analyticalsciencejournals.onlinelibrary.wiley.com/doi/10.1002/nbm.5159 by Joleen

McInnis -

· Deutsches Zentrum Für Neurodeg , Wiley Online Library on (108/08/2024). See the Terms and Conditions (https://onlinelibrary.wiley.com/terms-and-conditions) on Wiley Online Library for rules of use; OA articles are governed by the applicable Creative Commons License

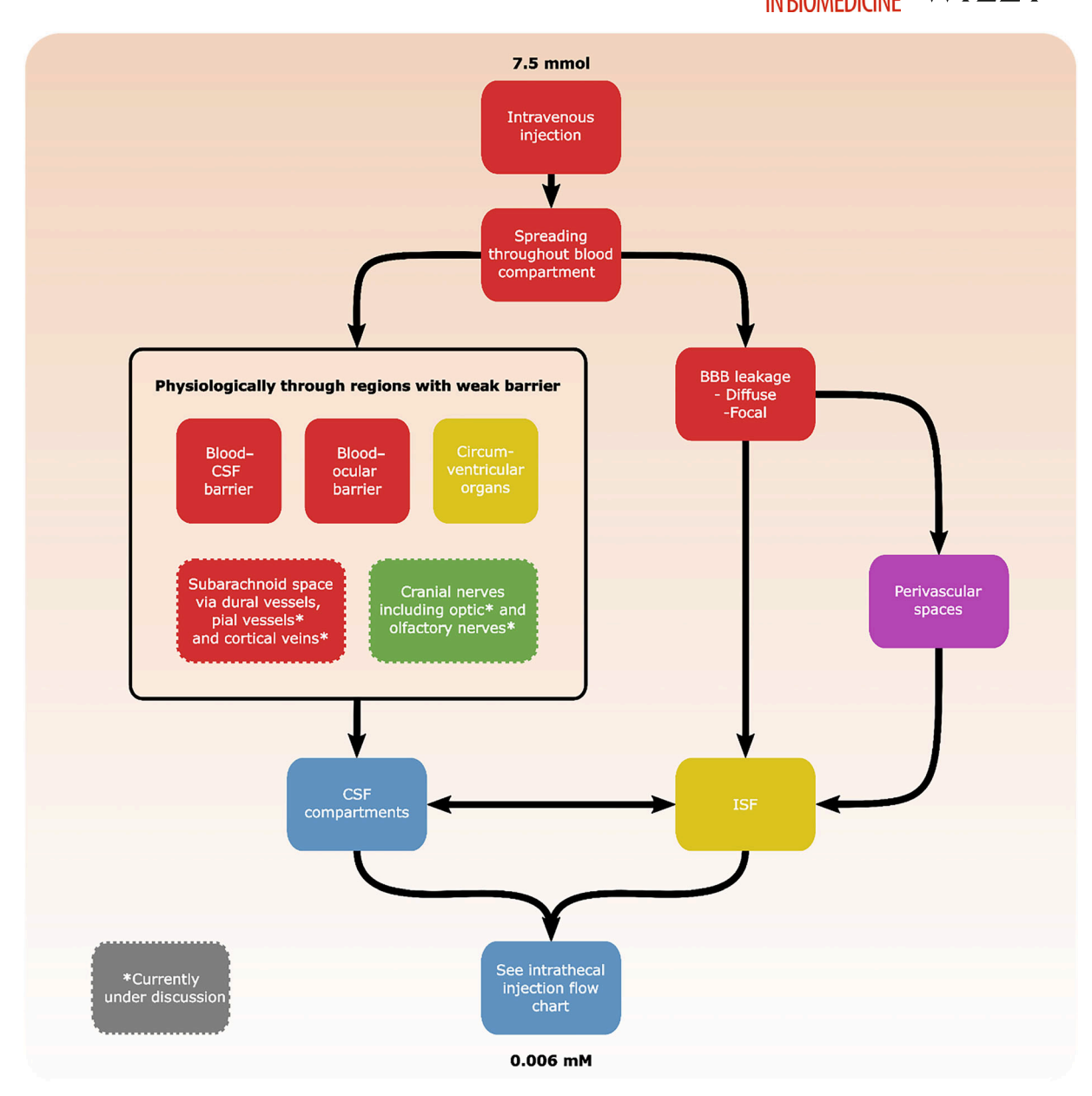


FIGURE 5 A schematic overview of pathways taken by intravenously injected contrast agent. Note that some of the contrast agent will reach CSF, ¹⁸ which can be seen as a crossover to the flowchart of intrathecal injections (see Figure 1). Colors have the same meaning as in Figure 1: blue boxes indicate large CSF spaces, green the lymphatic system, yellow interstitial spaces, purple spaces around vessels, and red the blood compartments. BBB, blood-brain barrier; CSF, cerebrospinal fluid; ISF, interstitial fluid; *, currently under discussion.

6 | INTRAVENOUS INJECTION PROTOCOL

There is less clear consensus on the intravenous injection protocol than for intrathecal injections, with the employed protocol frequently determined by other clinical or research scans that are dependent on the same contrast agent injection. This implies that the contrast agent is either injected with a power injector at a fast speed to allow dynamic susceptibility contrast (DSC) MRI perfusion measurements, ^{78,79} or is injected at a relatively slow injection speed for dynamic contrast-enhanced (DCE) MRI measurements of BBB integrity, ⁸⁰ or via manual injection. Similarly, the dose can differ, although a single dose (0.1 mmol/kg) is most common. ⁸¹ Assuming intravenous injection of 0.1 mmol/kg bodyweight of Gd-based contrast agent (these calculations were based on Gd-diethylenetriamipentacetate (Gd-DTPA) as an example, although this is no longer frequently used because of concerns about its stability ⁸²) and the use of a power injector, this would lead to a maximum concentration of approximately 6 mM in blood, settling around an equilibrium concentration of approximately 1–1.5 mM, and subsequently a washout with a half-life time of approximately 1.6 h for the elimination phase ⁸³ (Figure 7). The decrease in plasma concentration has traditionally been modeled by a bi-exponential function with a rapid distribution term, and a slow elimination term.

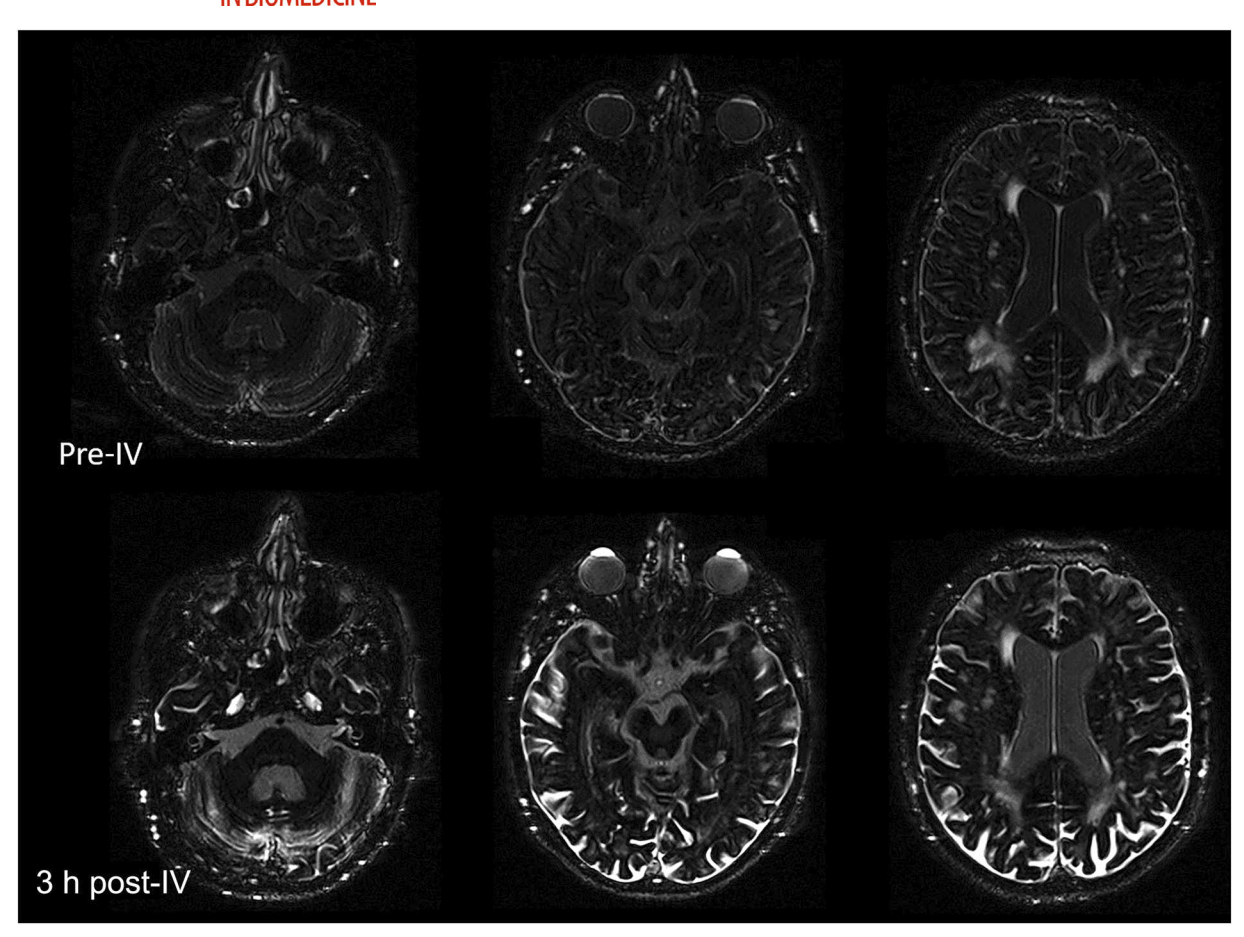


FIGURE 6 Contrast enhancement 3 h postintravenous injection (3 h post-IV, second row) on heavily T2-weighted FLAIR MRI compared with the noncontrast baseline scan (pre-IV, first row) in a subject without a diagnosed neurological condition showing relatively strong CA leakage into CSF. Contrast agent enhancement is visible throughout the SAS and ventricles, as well as Meckel's cave, cochlea, anterior eye chamber, vitreous, and SAS surrounding the distal optic nerve. Images scaled visually for optimal presentation. CA, contrast agent; CSF, cerebrospinal fluid; FLAIR, fluid-attenuated inversion recovery; SAS, subarachnoid space.

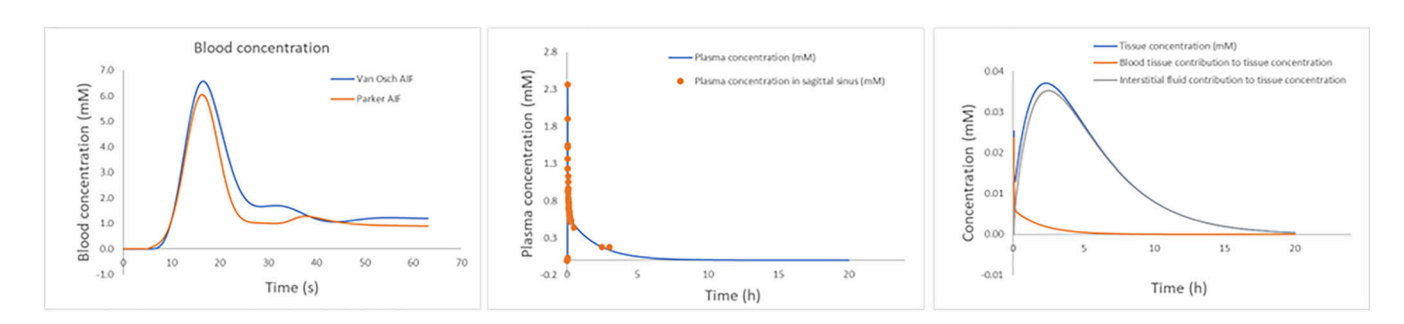


FIGURE 7 Concentration–time curves after an intravenous injection at t=0 s of a single dose of gadolinium (Gd). Left: first pass of the contrast agent followed by a small recirculation phase, upon which an equilibrium concentration is reached. Two curves are shown, one based on Parker et al., the other on van Osch et al., showing similar shapes and amplitudes. Highest Middle: plasma concentration measured in the superior sagittal sinus as well as the result of a bi-exponential fit (dose of 0.1 mmol/kg with \sim 1 min infusion time), calculated assuming a 0.45 hematocrit level. Right: tissue concentration as well as the contributions from interstitial fluid and intravascular compartments, simulated using the two-compartment extended Tofts model. Simulation parameters were a BBB leakage constant (Ki) of 1×10^{-3} min⁻¹, a 1% plasma volume fraction, and a 20% interstitial fluid volume fraction. At approximately 2.5 h the interstitial fluid contribution peaks, indicating the time when interstitial fluid and plasma concentrations are equal. Beyond this timepoint, interstitial fluid concentration is higher than that of plasma, leading to a reversal of net transport of Gd. Much sooner than this, however, the tissue concentration is dominated by the uptake in the interstitial fluid, rather than the intravascular contribution, because of the much larger volume of the former compartment. BBB, blood–brain barrier.

and-conditions) on Wiley Online Library for rules

of use; OA articles are governed by the applicable Creative Commons License

6.1 Crossing of the contrast agent across the BBB

Whereas contrast agent leakage as detected by DCE-MRI has been an important radiological marker for the diagnosis and staging of brain diseases, such as tumors, multiple sclerosis (MS), and inflammation, its usage in search of subtle BBB leakage has been introduced more recently. ⁸⁰ The BBB constitutes a semipermeable membrane that protects brain tissue by assuring that unwanted pathological substances and large bloodborne molecules cannot enter the CNS. However, subtle brain-wide leakage of Gd can occur across the capillary wall, which will cause detectable signal enhancements that can be disentangled from the vascular signal using compartment modeling. The capillary leakage rates are widely recognized to increase as a part of normal aging and are particularly pronounced in Apoe4 carriers. ⁸⁶

From the year 2003, the first studies were published that employed long duration DCE-MRI to detect subtle BBB damage in diabetes, AD, and small vessel disease. ^{87,88} Also, in normal aging, an increase in permeability over the BBB can be measured, albeit mainly limited to the hippocampus. ⁸⁶ When looking at reported average values of the unidirectional transfer constant K_i , these seem to be variable between studies, that is, values of the order of 1– 1.5×10^{-3} min⁻¹ were observed in the hippocampi of elderly subjects, K_i values of 2.8×10^{-4} min⁻¹ were measured in the WM in patients with early AD (increased with respect to normal subjects, who exhibited a K_i of 1.7×10^{-4} min⁻¹), and in vascular cognitive impairment (VCI) subjects a threshold of 3×10^{-4} min⁻¹ was used to discriminate healthy voxels in the WM from those in which the BBB was affected. ^{86,89,90} Indeed, quantifying weak BBB leakages appears challenging, with large variations in the reported values between different studies, calling for standardized protocols and postprocessing approaches. ⁹¹ A plurality of error sources has been identified, including the choice of injection protocol and discrepancies between the prescribed and the achieved flip angle. ⁹² Another limitation in the standard modeling of BBB leakage is that the effect of glymphatic flow is not explicitly modeled in, for example, Patlak analyses. It is conceivable that glymphatic flow leads to lower tracer concentrations in ISF, and therefore BBB leakage can be underestimated. When calculating with a K_i value of 1×10^{-3} min⁻¹ and the arterial input functions (AIFs) depicted in Figure 7 (left and middle panels), a maximum concentration of Gd of approximately 0.04 mM can be estimated in the brain tissue (Figure 7, right panel).

Several types of pathological lesions, for example, idiopathic normal pressure hydrocephalus, ⁹³ are associated with further BBB breakdown, of which WM lesions, a cardinal feature of small vessel disease, might be of particularly relevance for the purpose of studying brain clearance in an aging population. Observing WM lesions is a rule rather than an exception when neuroimaging elderly patients with postintravenous injection signal enhancements, reflecting that subtle BBB degradations show an association with WM lesion severity. ^{15,94}

6.2 | Spreading of the contrast agent across naturally weak barriers

Interestingly, contrast leakage from blood following intravenous injections is not limited to the brain tissue, but also involves contrast uptake directly into the CSF. The CSF enrichment likely occurs at multiple leakage points, involving leakage across the fenestrated vasculature of the choroid plexus, via blood–CSF interfaces in pial arteries and the venous vasculature in the SAS, and across other naturally weak barriers. 15,75,77,95,98 Based on experiments tailored to diagnose Meniere's disease, as well as on studies on Gd retention in the brain, it has been demonstrated that the contrast agent can be seen to enter CSF-filled spaces, 14,15 which was later confirmed by studies applying invasive CSF sampling. 18 These pioneering MRI studies have been made using FLAIR or heavily T_2 -weighting imaging several hours after Gd injection, whereas now quantitative imaging is being implemented to allow accurate estimation of CSF tracer concentrations. Initial data from these studies point towards average Gd concentrations within the SAS reaching approximately 3 μ M following a standard dose of 0.1 mmol/kg at approximately 3 h postinjection, 99 and therefore being orders of magnitude lower compared with those following the intrathecal protocols described above. Interestingly, Cao et al. reported Gd concentrations in CSF of approximately 0.2 mM, 100 estimated from signal drop on an optimized T_2 -dominant 3D turbo spin echo (TSE) sequence. This would correspond to a Gd concentration of approximately one-fifth of the concentration in the blood. However, the reported signal changes were measured close to the dura and might therefore present focal peak signal changes due to the penetration of Gd from BBB-lacking dural blood vessels or cortical veins into the CSF.

Several entry pathways of contrast agent to the CSF spaces have been suggested and are outlined below.

6.2.1 | Spreading of the contrast agent into the SAS

Intravenously administered contrast agent was shown to appear early in the CSF of the SAS. 99-101 As dural vessels are known to lack a blood-CSF barrier 102,103—wherefore the dura shows a strong and early maximum enhancement 30 min postinjection 104—dural vessels might be a source of early Gd uptake of the SAS. Furthermore, pial vessels within the SAS were proposed to be a site of blood-CSF water exchange and are known to be more permeable for smaller sized solutes as well as in the pathologic state, 26,105 and might be an additional entry point of Gd into the SAS. Additionally, Gd was shown to accumulate in the SAS around cortical veins, especially in subjects aged older than 37 years, and pial venules and veins were determined as primary sites of BBB disruption following acute hypertension. 77,106 Importantly, Absinta et al. reported diffuse dural

0991492, 2024, 9, Downloaded from https://analyticalsciencejournals.onlinelibrary.wiley.com/doi/10.1002/nbm.5159 by Joleen McInnis - Deutsches Zentrum Für Neurodeg, Wiley Online Library on [08/08/2024]. See the Terms

enhancement in combination with tubular enhancing structures that they interpreted as meningeal lymphatic vessels. ¹⁰⁷ This is an interpretation that needs to be validated in further studies, because the dura in this region also has a rich network of blood vessels. Last, but not least, Freeze et al. described focal pericortical CSF enhancement on postcontrast FLAIR images as an unspecific imaging sign in approximately 28% of all investigated cases, including AD, mild cognitive impairment, and healthy controls. In their study, focal CSF enhancement correlated with age and ischemic injury, but not with cognition or diagnosis group. ¹⁰⁸

6.2.2 | Spreading of the contrast agent into ventricular CSF

Different studies in humans and rodents suggest penetration of Gd via the fenestrated vasculature of the choroid plexus into the CSF of the ventricles. 15,95 Accordingly, Richmond et al. report on a maximum signal intensity increase of the choroid plexus 30 min postinjection. 104 While the signal–time curve of the choroid plexus depicted a dynamic evolution equivalent to that of the venous and arterial vasculature—and therefore most likely represents vascular signal—it was accompanied by a rapid and marked signal intensity increase of the lateral ventricles, which suggests penetration of Gd via the fenestrated vessels of the choroid plexus into the CSF. 104 Using intravenous injections and serial T_1 -mapping, it was reported that ventricular CSF Gd concentration develops similarly to that of the SAS, without any apparent lead–lag relationship between the two compartments. 99

6.2.3 | Spreading of the contrast agent into perivascular CSF

Contrast enhancement was shown to occur in the fluid-filled, MRI-visible PVS within the basal ganglia (BG), ^{15,109} which have been shown to serve as a marker of small-vessel disease. ¹¹⁰ It is known that MRI-visible PVS primarily seem to mainly consist of periarterial PVS and therefore are supposed to represent the entry route of the glymphatic system. ¹¹¹ However, the exact pathway Gd takes from the intravascular compartment towards the PVS remains unclear. Gd could either enter from the SAS following the perivascular route, or Gd within the PVS could represent subtle Gd leakage across the arteriolar wall.

Remarkably, while contrast enhancement was described for PVS in the BG, no such enhancement was found for PVS in the WM, which led the authors to suggest a different fluid composition and/or clearance function of the different PVS.¹¹² Known regional differences of PVS' anatomical structure, as well as differences in association with risk factors and pathologies, might also contribute to different contrast enhancement patterns.^{113,114} Naganawa et al. described a giant perivascular space in the BG without any contrast enhancement on delayed FLAIR after intravenous Gd administration.¹¹⁵

6.2.4 | Spreading of the contrast agent across the blood-ocular barrier

Signal enhancement of the inner eye drew attention to Gd extravasation into the eye bulb, presumably mediated by the blood-ocular barrier, which has a higher permeability than the BBB. As this enhancement was accompanied by an enhancement of the SAS surrounding the distal optic nerve, intravenous Gd injection was suggested to visualize the ocular glymphatic system, which clears amyloid- β from the highly metabolically active retina. 116,117

Specifically, at least two locations of intraocular penetration were reported: the anterior eye chamber as well as the orra serrata's inferior temporal side. However, to what extent the different parts of the blood-ocular barrier contribute to intraocular Gd penetration, and how much of the Gd is actually drained via the posterior pathway instead of the Schlemm's canal, is currently unknown. Remarkably, other studies reporting on Gd distribution along intracranial nerves (inter alia within Meckel's cave and the inner auditory canal) propose an alternative reason for the enhancement of the optic nerve. 118

Ocular MRI following intravenous Gd administration can serve as a diagnostic imaging tool in patients suffering from different eye pathologies. For example, in children with retinoblastoma, enhancement of the anterior eye chamber predicted optic nerve infiltration. 117,119 Furthermore, ocular Gd distribution following intravenous injection differed between pathologies of the anterior compared with the posterior eye segment, probably due to disruption of different parts of the blood-ocular barrier. 120

6.2.5 | Spreading of the contrast agent through the cribriform plate

There is a proposed CSF clearance route spanning the olfactory nerve, exiting the brain at the cribriform plate and entering the lymphatic circulation of the nasal mucosa. However, more research is needed to gain further understanding of this clearance route in humans. While this

0991492, 2024, 9, Downloaded from https://analyticalscie

ournals onlinelibrary, wiley, conduction 1002/bbm, 3159 by Joleen McInnis - Deutsches Zentrum Für Newcodeg, Wiley Online Library on [08/08/2024], See the Terms and Conditions (https://onlinelibrary.wiley.com/terms-and-conditions) on Wiley Online Library for rules of use; OA articles are governed by the applicable Creative Commons License

pathway serves as a major CSF efflux route within multiple animal species, with an estimated clearance ratio of up to 50% of the produced CSF, ¹²³⁻¹²⁶ its relevance in human brain clearance has not been fully elucidated. Signal enhancement in the CSF regions around the cribriform plate in FLAIR images from human subjects can be observed within 20–30 min postinjection. ¹²⁷ However, the signal intensity changes close to the basal routes (cribriform plate and jugular foramina) were smaller than that observed around the superior sagittal sinus (67% compared with 82%–119%), as well as less uniform and more diffuse compared with the focal pattern around the superior sagittal sinus. The authors concluded that the enhancement could represent contrast agent in different compartments (fluid spaces, connective tissue, lymphatics) and that the fluid pathway remains unclear.

6.2.6 | Spreading of the contrast agent along cranial nerves

Besides the optic and olfactory nerves, other cranial nerves have also attracted attention as possible CSF outflow routes.⁴ Signal enhancement after intravenous injection of Gd has been demonstrated in CSF spaces surrounding cranial nerves, such as the SAS surrounding the optic nerve, the Meckel's cave inhabiting the trigeminal ganglion, the internal auditory canal, as well as the cochlear perilymph surrounding the vestibulocochlear nerve with peak signal intensities within the first 4.5 h postinjection.^{15,98,104,120,128} Furthermore, Varatharaj et al. used the focal BBB breakdown in a MS brainstem lesion to simulate intraparenchymal administration of Gd.¹²⁹ After intravenous injection of the contrast agent, the proximal trigeminal nerve, which is devoid of a vascularized perineurium and epineurium, depicted an enhancement pattern similar to the brain parenchyma surrounding the MS lesion, while the signal enhancement within the peripheral part of the nerve resembled the vascular driven enhancement of the MS lesion. These results were interpreted as continuity between the ISF space within the brainstem and the proximal trigeminal nerve, suggesting a cranial nerve drainage pathway.

6.2.7 | Spreading of the contrast agent around the circumventricular organs

The circumventricular organs occupy specific areas within the walls of the third and fourth ventricle, which physiologically lack a BBB. Therefore, theoretically, the circumventricular organs are predestined to enable leakage of contrast agent into the CSF. It was shown that the organum vasculosum of the lamina terminalis showed enhanced signal intensity after intravenous injection of Gd, with a signal intensity peak at 30 min postinjection, and a steady decline thereafter.¹³⁰

7 | COMPARISON OF THE HUMAN SITUATION WITH ANIMAL MODELS

Animal studies have paved the way for groundbreaking discoveries in the field of brain clearance at both an anatomical and functional level, where high-resolution imaging such as two-photon microscopy and experimental interventions enable studies that are beyond reach in humans. The human studies have confirmed that CSF influx occurs primarily along the PVS surrounding the large cerebral arteries. 16 and that clearance of contrast agent from the brain parenchyma is accelerated by sleep. 34 Nevertheless, substantial structural species differences exist that justify further research that aims to translate the laboratory findings to the clinic. Compared with the much smaller and smoother surface of the lissencephalic murine brain, the human gyrencephalic brain has a substantially different anatomy, leading to more complex patterns of CSF flow. Whereas CSF tracer enhancement and clearance in the rodent brain were typically observed over a time scale of a few hours, similar patterns of CSF tracer pharmacokinetics within the intracranial compartment occur over days in humans. A study in pigs demonstrated that the density of PVS in the cerebral cortex was up to four times higher than that in rodents, suggesting a similarly high density in humans. 131 In addition to the fundamental anatomical differences, physiological differences between animals and humans must be considered when studying the glymphatic system. For example, cardiac- and respiration-related pulsatile cycles, which are considered to be key drivers of glymphatic flow, 132,133 differ between rodents and humans up to an order of magnitude. 134 The volume, production rate, and turnover of CSF are also enormously different. 135 These physiological differences may affect the pattern of tracer distribution more than what can be expected only from different anatomical features. Moreover, the difference in body posture should also be considered to be a factor influencing the intracranial pressure. 136,137 Successful translation of findings between rodents and humans will require computational/mathematical models that take into account these anatomical and physiological differences.3 Whereas CSF efflux through the cribriform plate to the nasal lymphatics plays a major role in rodents, such efflux was hardly detected in humans with intrathecally injected contrast agents, 65 although enhancement was observed after intravenous injections. 127 These differences may be related to the entry point of the contrast agent (cisterna magna in rodents vs. lumbar spine in humans), which could lead to less contrast agent being evacuated from the more peripheral injection points as employed in humans. A human dynamic positron emission tomography study provided some evidence of CSF clearance along olfactory nerves, ¹³⁸ but in the future, technical improvements are necessary to bridge this translational research gap.

7.1 | Intrathecal injections to monitor brain clearance

Methodological differences of intrathecal tracer studies also exist between species. In rodents, the tracer is mainly injected into the cisterna magna in an amount that, by percentage of the intracranial CSF volume, is much higher than with intrathecal injections in humans. Although it has been reported that most rodent injection protocols do not affect CSF influx or intracranial pressure, they do require careful injections so as not to manipulate intracranial physiology, especially to not increase intracranial pressure. The CSF tracer typically distributes in the cisterns at the base of the rodent brain, and the amount of tracer reaching the intracranial compartment is, therefore, more predictable with injections directly into the cisterna magna. In humans, injections of fluid at the lumbar level, in amounts of up to typically 1 mL, have no theoretical influence on intracranial pressure or CSF flow. There are, however, individual differences in spinal transit time, having the consequence that the timing of tracer entry into the intracranial compartment is less predictable. Furthermore, a substantial resorption of the tracer from the spinal canal also results in variations regarding how much of the injected tracer reaches the intracranial CSF space.

8 | DISCUSSION

More than a decade since the first description of the glymphatic system⁴, research on human brain clearance imaging can still be considered as being at an early phase of development. This review has focused on two main MRI concepts with which to study glymphatic function, both based on utilizing Gd-based contrast agents as tracers: direct insertion into the CSF using intrathecal injections and intravenous injections that deliver Gd to the brain tissue through several potential pathways. For the first time, we have provided an overview of the path taken by this exogenous tracer and the typical concentration profiles of the two approaches. Important differences between the two approaches involve the safety profile of the type of injection, the effective concentration differences between the involved compartments, and the exact insight that each technique provides on the glymphatic system. Finally, we discuss the current challenges and knowledge gaps of both techniques, that is, the need for future research.

The clear disadvantage of intrathecal injections is the need for a lumbar puncture with the associated potential side effects, although these side effects are well understood and treatment is rather standard. A second concern could be that intrathecal injections could increase the Gd retention in the brain. However, we showed previously in this review that peak Gd concentrations in brain tissue after an intravenous and an intrathecal dose are of the same order of magnitude. To this end, no signs of Gd retention have been observed in human brains 4 weeks after intrathecal administration of 0.5 mmol of gadobutrol. 3 Subsequently, it was previously shown that an intrathecal dose of 0.25 mmol is sufficient to provide good image quality at 1.5-T MRI, while a body dose in an 80-kg subject after intravenous administration is typically 8 mmol (0.1 mmol/ kg), that is, 32 times higher. Regarding concerns with neurotoxicity from intrathecal administrations, a meta-analysis of 1036 cases showed no serious adverse effects for doses of 1.0 mmol or less. 41 Additionally, 346 patients were prospectively included in studies investigating the safety of intrathecal injections of gadobutrol for doses of 0.5 mmol or less, demonstrating a favorable safety profile, and no serious side effects. 32,39,40 In line with recommendations for intravenous use, linear MRI contrast agents should also be avoided intrathecally. We would like to emphasize that gadobutrol is currently the only macrocyclic Gd-based contrast agent where prospective safety studies of its intrathecal use have been carried out. Conceptually, the use of contrast agents with different molecule sizes could be highly interesting as, for example, demonstrated in animal studies. 140 The final concern could be that intrathecal administration of Gd-based contrast agents is off-label. However, it should be emphasized that off-label use of drugs in general is not rare in clinical practice, and that regulatory agency approval is a marker of increased certainty about safety, whereas an absence of approval does not necessarily imply not being safe. When physicians use a product for an indication not in the approved labeling, they are responsible for being well informed about the product, base its use on firm scientific rationale and sound medical evidence, and to register the product's use and effects. Increased safety measures with intrathecal use of a Gd-based contrast agent can be achieved by use of the lowest diagnostic dose, a syringe with a maximum size of 1 mL (i.e., 0.25 mL of gadobutrol and 0.75 mL of saline), and slow injection rates. Of course, all procedures need to adhere to the European Society of Urogenital Radiology (ESUR) safety guidelines, including the collection of informed patient consent.

The safety profile of intravenous injections is well known and therefore requires little discussion. Maybe one exception to this is the advised injection speed. Assuming that the injection is done within the MRI scanner, it is advised to combine the injection with a DCE experiment aimed at measuring subtle BBB damage and therefore to tune the injection speed to this specific goal. Acquiring such a scan would provide important background information on the amount of contrast agent entering the neuropil, which can be considered the input function for the brain clearance scans acquired at later timepoints. This will remain important information until we better understand the intersubject variations and thus how to interpret intravenous brain clearance scans. Another point of uncertainty is the hematocrit, especially in the capillaries, which both influences the cerebral perfusion and determines the concentration difference between plasma and the extravascular compartment.

Because of the different injection sites, the concentration profiles in the involved compartments will differ dramatically between the two approaches. For intrathecal injections, the assumption is that the Gd-tracer movement is dominated by the bulk flow of CSF and accordingly first distributes throughout the CSF system, followed by entering brain tissue, and subsequently being cleared from the brain and CSF, where brain

clearance appears to be dependent upon CSF clearance. Human imaging with intrathecal gadobutrol has indeed clearly demonstrated the distribution of the tracer into the subarachnoid cisterns at the base of the skull, after which distribution in the antegrade direction along the large artery trunks within the major cerebral fissures occurs. Subsequently, CSF-ISF exchange occurs centripetally from the cortical surface, mainly in the cortex, only to a limited extent in WM regions immediately beneath the cortex, and to an almost negligible extent in deep WM regions. Significant concentration gradients on CSF-tissue interfaces make it challenging to differentiate ISF and CSF concentrations directly at the cortex, whereas deeper into the cortex this differentiation can be reliably made. It also implies that because little contrast agent is reaching the deep WM, the intrathecal approach is less well suited for studying clearance from deep WM regions. However, it should be emphasized that the glymphatic system was described in vivo as a clearance pathway within the cortex, and the primary aim of brain clearance imaging in light of neurodegenerative diseases should be to find surrogate measures for the clearance of neurotoxic endogenous solutes from the cortex, where many of these disabling diseases primarily occur.

For intravenous injections, only a small proportion of the injected contrast agent will enter the extravascular brain tissue compartment, as can also be concluded from the fact that Gd is still called an intravascular tracer. This implies that a highly significant concentration difference needs to be present between blood and ISF compartments to promote leakage into the tissue. From the simulations depicted in Figure 7, it can be concluded that, after only 2.5 h, the concentration of Gd in the blood and tissue compartments equalize, after which the effective direction of contrast agent movement will shift from tissue towards blood. Because of the smaller volume of the vasculature compared with the interstitial volume, the relative contribution to the tissue signal will already be dominated by the interstitial component before this timepoint. However, one should realize that identifying the ISF concentration and differentiating it from blood concentrations remains very challenging, especially with subtle BBB leakage. Studies using the intravenous approach have interpreted contrast enhancement in WM as a sign of CSF-ISF exchange, however, at much earlier timepoints than was observed with intrathecally enhanced MRI, which showed that up to 24 h may pass before CSF exchanges into deep WM. Concentration-time curves in these studies seem to resemble the pharmacokinetic profile of Gd in blood, whereas the profiles of tissue and CSF will be even more similar, making differentiation of these compartments difficult. Therefore, it will be very easy to misinterpret enhancement in brain tissue as CSF-ISF exchange, instead of leakage over the BBB. The acknowledgment that intravenous contrast agents leak directly both into CSF and into brain tissue over the capillary wall will thus further complicate any analysis. Therefore, based upon only the T₁ shortening of brain tissue, it is impossible to conclude from which leakage pathway this shortening is caused.

Finally, both approaches are hindered by our still limited knowledge on the human anatomy and in vivo functioning of the glymphatic system. For example, the potential impact of various membranes, such as the subarachnoid lymphatic-like membrane layer, 48 with each layer having different permeabilities, is not fully known, but will presumably influence the spread of contrast agent in the CSF compartment, as well as the penetration of contrast agent into the brain tissue. More dense sampling, both temporally and spatially, might help to gain more insight into this.

The last topic to discuss when comparing the two approaches is the insight into the brain clearance system that is provided by the two techniques. When going back to the basics of tracer kinetics as, for example, described by Lassen, 141 it is clear that any proper characterization of a system depends on a well-defined and quantified input function in combination with a measurement at the outlet or of the amount of tracer residing in the tissue of interest. When considering the input function, then one would ideally insert the tracer directly into the extravascular brain tissue compartment without disturbing the local conditions, such as the pressure. This is also an active discussion in rodent experiments, which led, for example, to a dual-syringe system injecting tracer into the cisterna magna while withdrawing an equal amount at the same moment, 142 or to local delivery of tracer by disrupting a blood vessel. 143 However, whereas in the first example injection is still performed outside of the neuropil into the cisterna magna, the second approach is disruptive to the local system. When comparing the intrathecal and intravenous approaches in humans, entrance of contrast agent is achieved into the neuropil when intravenously injected agents cross the BBB and thus at the exact location of the ideal input function. However, the amount of leaked contrast agent is very dependent on the local condition of the BBB. This last limitation is especially troublesome, because BBB breakdown and impaired brain clearance are both thought to be involved in neurodegeneration. Moreover, entrance via the BBB is only one of the many entrance points into the extravascular compartments of our cranium. Therefore, a clear input function is lacking. This is opposed to the intrathecal approach, in which a clear point of entrance into the system is present. This entrance point is, however, downstream of the system that we want to study, and the contrast agent first has to be distributed throughout the CSF system and into the brain before the clearance phase can be studied. However, because the input of tracer is much clearer, leading to a much better-defined cascade of spreading and clearance phases (see Figure 1 and compare with Figure 5), we confidently declare the intrathecal approach the currently preferred approach of human brain clearance imaging. Regarding measurement of tracer retention or outflow, both approaches frequently rely on qualitative observations, thereby limiting the possibility of quantitative tracer kinetic analysis. Qualitative observations in the context of brain clearance are especially difficult, because images are obtained at an interval of a few hours, that is, during different scan sessions. Unfortunately, MRI scanners are not built as quantitative measurement devices, and subsequent sessions can result in different scaling of images, for example, due to different power optimization, reference scans, and positioning within the coil. Finding proper regions for calibrating the signal is difficult, because in the end the contrast agent reaches almost all of the MR signal-producing regions within the cranium. Quantitative measurements based upon T₁ relaxation times may resolve many of these concerns, although quantification is more time consuming and also involves auxiliary measurements, such as B₁, whose measurement errors will subsequently translate to errors in the quantitative values.

The last topic on quantitative versus qualitative measurements is therefore also our first recommendation for future research. Improved quantification, and preferably measurements with shorter time intervals, would improve our understanding of the pharmacokinetics and would improve our understanding of the many interrelated elements incorporated by the human perivascular brain clearance system (see Figures 1 and 5).

However, quantitative T_1 measurements should only be considered a first step. The next step is even more complex and would involve somehow capturing the glymphatic function in a single quantitative marker, similar to the filtration rate that is used for kidney function. Even better would be when such a number could be calculated for different brain regions or could even be summarized into a quantitative map depicting regional glymphatic efficiency. When looking at the intersubject differences in enhancement patterns in Figure 2 and the multiple entry points of the intravenously injected contrast agent into the glymphatic system, this task might be considered too complex with currently available tools. Thus, we recommend first to better understand the studied system, as well as the intersubject variations, before aiming to summarize the complex dynamics into a single number. Moving too early to a single number has the risk of oversimplifications that might lead to misinterpretation or premature rejection of these new approaches due to negative or conflicting findings.

It is important to consider that both methods rely upon injection of a contrast agent, and literature on CE brain clearance imaging in healthy subjects is scarce and overwhelmed by data in patients suffering from neurovascular disorders, potentially creating a bias in our understanding. Therefore, and also for increasing the general applicability, the availability of noninvasive alternatives would be highly beneficial. Noninvasive methods rely mainly on imaging the solvent of the glymphatic system, that is, the CSF and ISF. Whereas these techniques are attractive because of their noninvasive nature, they do not reflect the movements of larger solutes and are therefore not providing insights into how these are traversing the glymphatic system over hours and days. Moreover, several of these techniques focus on the WM, which is not the main production or accumulation site of neuronal waste, or the primary site of neurodegeneration. However, noninvasive approaches can be very helpful in understanding subparts of the glymphatic system, especially because they enable characterizing CSF/ISF dynamics with a much shorter temporal footprint and thereby, for example, allow studying how the cardiac and respiratory cycle, as well as vasomotion, affect the mobility of CSF/ISF, which might in turn affect the clearing efficiency. In our opinion, all these imaging approaches need to be studied further to complete our understanding of the human brain clearance system. We do, however, want to caution on the use of diffusion tensor image analysis along the perivascular space (DTI-ALPS) as a pure measure of brain clearance: this approach does not isolate CSF or ISF signal; moreover, it is dependent on anatomical assumptions, and is only measuring properties at a single location.⁵⁰ Whereas currently a vast amount of publications are published, as this approach can be performed retrospectively on previously acquired DTI data, these also have a high risk of bias: mainly positive results are published, with the risk that due to self-censoring or reviewers' concerns, negative results do not make it into the literature. Further validation of DTI-ALPS is required before the ALPS index can be considered to be a surrogate marker of glymphatic function. This could already be deduced from our concerns on developing a single summarizing parameter out of intravenous or intrathecal contrast-enhanced MRI: it seems too early to simplify this complex, incompletely understood system into a single number. Other noninvasive approaches that are being pursued include, for example, measurements based on arterial spin labeling (ASL). It should be noted that these mainly monitor water transport across the BBB or from blood-to-CSF, and therefore only provide information on a small, although potentially important, part of the brain clearance system. Interestingly, these phenomena can also be studied with O17-H2O MRI, which provides a completely complementary viewpoint to the Gd-based contrast agent for probing the brain clearance system and has the advantage over ASL that it does not suffer from fast decay times. 144,145 The diffuse, and not centripetal, enhancement of intrathecally injected O17-H2O in one study may suggest that water is quickly resorbed by blood vessels and recirculated into brain, 146 which may be corroborated by the observations of large, continuous water fluxes over the vessels wall by ASL. 26 Also, the magnetic resonance encephalography (MREG) technique pioneered by the Oulu group has, via noninvasive neuroimaging, been able to replicate key features of glymphatic flow originally described in preclinical studies, including the importance of vascular pulsatility (heart rate and slow vasomotion), ¹³³ sleep dependence, ¹⁴⁷ and dysfunction in AD. ¹⁴⁸

Finally, we want to reiterate the recycling of Gd-based contrast agents between both of the approaches discussed: after intrathecal injections, tracer ends up in the bloodstream, bridging over to the systemic circulation, albeit at low concentrations. Similarly, intravenously injected contrast agent enters the CSF and thus directly transposes to the intrathecal pathways. It should, however, be emphasized that, whereas in the end exactly the same compartments are reached, the relative difference in concentrations determines the ability of each method to differentiate and characterize certain parts of the glymphatic system. With both of these approaches, and potentially in combination with noninvasive approaches that are not the topic of the current review, human brain clearance imaging is now firmly established, with many in vivo data already available. These approaches will provide us with the knowledge with which to improve our understanding of the glymphatic system and how it is affected by neurological diseases.

ACKNOWLEDGMENTS

This review was funded by the HCBI project. The HCBI-project ("Human brain clearance imaging: a window on physiological disturbances in the prediagnostic phase of neurodegenerative diseases") is an EU Joint Programme–Neurodegenerative Disease Research (JPND) project. The project has received funding from the European Union's Horizon 2020 Research and Innovation Programme under grant agreement No. 825664. Additional funding was received by Alzheimer Netherland (MJPvO, LH), Netherlands Organisation for Scientific Research (NWO) (MJPvO, project

M20-238), Swedish Research Council (AW, 2022-04263), the Swedish Foundation for Strategic Research (AE), and The Research Council of Norway (RCN) (GAR, project 333956).

CONFLICT OF INTEREST STATEMENT

Matthias van Osch reports research support from Philips. Alexander Radbruch reports past financial study support from Bayer and Guerbet, and personal fees from Bayer and Guerbet. Katerina Deike reports past financial study support from Bayer and Guerbet, and personal fees from GE. Maiken Nedergaard is a consultant for CNS2. Per Kristian Eide and Geir Ringstad are shareholders in BrainWideSolutions AS, Oslo, Norway, which is a holder of patent US 11272841. Geir Ringstad has received a speaker fee from Bayer AG, Berlin, Germany.

ORCID

Matthias J. P. van Osch https://orcid.org/0000-0001-7034-8959

Anders Wåhlin https://orcid.org/0000-0001-6784-1945

Ingrid Mossige https://orcid.org/0009-0009-3342-8592

Lydiane Hirschler https://orcid.org/0000-0003-2379-0861

Anders Eklund https://orcid.org/0000-0002-2031-722X

Klara Mogensen https://orcid.org/0009-0004-6341-8444

Ryszard Gomolka https://orcid.org/0009-0001-9797-1062

Alexander Radbruch https://orcid.org/0000-0001-6238-6525

Sara Qvarlander https://orcid.org/0000-0002-1454-4725

Andreas Decker https://orcid.org/0009-0009-6018-3666

Maiken Nedergaard https://orcid.org/0000-0001-6502-6031

Yuki Mori https://orcid.org/0000-0003-4208-0005

Per Kristian Eide https://orcid.org/0000-0001-6881-9280

Katerina Deike https://orcid.org/0000-0002-4319-0428

Geir Ringstad https://orcid.org/0000-0003-0919-4510

REFERENCES

- 1. Agarwal N, Lewis LD, Hirschler L, et al. Current understanding of the anatomy, physiology, and magnetic resonance imaging of neurofluids: update from the 2022 "ISMRM Imaging Neurofluids Study group" workshop in Rome. *J Magn Reson Imaging*. 2023;59(2):431-449. doi:10.1002/jmri.28759
- 2. Koemans EA, Chhatwal JP, van Veluw SJ, et al. Progression of cerebral amyloid angiopathy: a pathophysiological framework. *Lancet Neurol.* 2023; 22(7):632-642. doi:10.1016/S1474-4422(23)00114-X
- 3. Bohr T, Hjorth PG, Holst SC, et al. The glymphatic system: current understanding and modeling. *iScience*. 2022;25(9):104987. doi:10.1016/j.isci. 2022.104987
- 4. Iliff JJ, Wang M, Liao Y, et al. A paravascular pathway facilitates CSF flow through the brain parenchyma and the clearance of interstitial solutes, including amyloid β. Sci Transl Med. 2012;4(147):147ra111. doi:10.1126/scitranslmed.3003748
- Iliff JJ, Goldman SA, Nedergaard M. Implications of the discovery of brain lymphatic pathways. Lancet Neurol. 2015;14(10):977-979. doi:10.1016/ S1474-4422(15)00221-5
- 6. Xie L, Kang H, Xu Q, et al. Sleep drives metabolite clearance from the adult brain. Science. 2013;342(6156):373-377. doi:10.1126/science.1241224
- 7. Carare RO, Bernardes-Silva M, Newman TA, et al. Solutes, but not cells, drain from the brain parenchyma along basement membranes of capillaries and arteries: significance for cerebral amyloid angiopathy and neuroimmunology. *Neuropathol Appl Neurobiol.* 2008;34(2):131-144. doi:10.1111/j. 1365-2990.2007.00926.x
- 8. Aldea R, Weller RO, Wilcock DM, Carare RO, Richardson G. Cerebrovascular smooth muscle cells as the drivers of intramural periarterial drainage of the brain. *Front Aging Neurosci.* 2019;11:1. doi:10.3389/fnagi.2019.00001
- 9. Weller RO, Djuanda E, Yow HY, Carare RO. Lymphatic drainage of the brain and the pathophysiology of neurological disease. *Acta Neuropathol.* 2009;117(1):1-14. doi:10.1007/s00401-008-0457-0
- 10. Louveau A, Plog BA, Antila S, Alitalo K, Nedergaard M, Kipnis J. Understanding the functions and relationships of the glymphatic system and meningeal lymphatics. *J Clin Invest.* 2017;127(9):3210-3219. doi:10.1172/JCI90603
- 11. Louveau A, Herz J, Alme MN, et al. CNS lymphatic drainage and neuroinflammation are regulated by meningeal lymphatic vasculature. *Nat Neurosci.* 2018;21(10):1380-1391. doi:10.1038/s41593-018-0227-9
- 12. Tarasoff-Conway JM, Carare RO, Osorio RS, et al. Clearance systems in the brain-implications for Alzheimer disease. *Nat Rev Neurol.* 2015;11(8): 457-470. doi:10.1038/nrneurol.2015.119
- 13. Sigurdsson B, Hauglund NL, Lilius TO, et al. A SPECT-based method for dynamic imaging of the glymphatic system in rats. *J Cereb Blood Flow Metab*. 2023;43(7):1153-1165. doi:10.1177/0271678X231156982
- Naganawa S, Yamazaki M, Kawai H, Bokura K, Sone M, Nakashima T. Visualization of endolymphatic hydrops in Ménière's disease with single-dose intravenous gadolinium-based contrast media using heavily T(2)-weighted 3D-FLAIR. Magn Reson Med Sci. 2010;9(4):237-242. doi:10.2463/mrms. 9.237
- 15. Deike-Hofmann K, Reuter J, Haase R, et al. Glymphatic pathway of gadolinium-based contrast agents through the brain: overlooked and mis-interpreted. *Invest Radiol.* 2019;54(4):229-237. doi:10.1097/RLI.000000000000033

0991492, 2024, 9, Down

McInnis

Deutsches Zentrum Für Neurodeg,

- 121537. doi:10.1172/jci.insight.121537
- JCI Insight. 2021;6(9):147063. doi:10.1172/jci.insight.147063

- 21. Sakka L, Coll G, Chazal J. Anatomy and physiology of cerebrospinal fluid. Eur Ann Otorhinolaryngol Head Neck Dis. 2011;128(6):309-316. doi:10. 1016/j.anorl.2011.03.002
- 22. Hodel J, Lebret A, Petit E, et al. Imaging of the entire cerebrospinal fluid volume with a multistation 3D SPACE MR sequence: feasibility study in patients with hydrocephalus. Eur Radiol. 2013;23(6):1450-1458. doi:10.1007/s00330-012-2732-7
- Ekstedt J. CSF hydrodynamic studies in man. 2. Normal hydrodynamic variables related to CSF pressure and flow. J Neurol Neurosurg Psychiatry. 1978;41(4):345-353. doi:10.1136/jnnp.41.4.345
- 24. Brown PD, Davies SL, Speake T, Millar ID. Molecular mechanisms of cerebrospinal fluid production. Neuroscience. 2004;129(4):957-970. doi:10. 1016/j.neuroscience.2004.07.003
- 25. Nigrovic LE, Kimia AA, Shah SS, Neuman MI. Relationship between cerebrospinal fluid glucose and serum glucose. N Engl J Med. 2012;366(6): 576-578. doi:10.1056/NEJMc1111080
- 26. Petitclerc L, Hirschler L, Wells JA, et al. Ultra-long-TE arterial spin labeling reveals rapid and brain-wide blood-to-CSF water transport in humans. Neuroimage. 2021;245:118755. doi:10.1016/j.neuroimage.2021.118755
- 27. Liu G, Ladrón-de-Guevara A, Izhiman Y, Nedergaard M, Du T. Measurements of cerebrospinal fluid production: a review of the limitations and advantages of current methodologies. Fluids Barriers CNS. 2022;19(1):101. doi:10.1186/s12987-022-00382-4
- 28. Mathiisen TM, Lehre KP, Danbolt NC, Ottersen OP. The perivascular astroglial sheath provides a complete covering of the brain microvessels: an electron microscopic 3D reconstruction. Glia. 2010;58(9):1094-1103. doi:10.1002/glia.20990
- 29. Eide PK, Ringstad G. MRI with intrathecal MRI gadolinium contrast medium administration: a possible method to assess glymphatic function in human brain. Acta Radiol Open. 2015;4(11):2058460115609635. doi:10.1177/2058460115609635
- 30. Yang L, Kress BT, Weber HJ, et al. Evaluating glymphatic pathway function utilizing clinically relevant intrathecal infusion of CSF tracer. J Transl Med. 2013;11:107. doi:10.1186/1479-5876-11-107
- 31. Ringstad G, Vatnehol SAS, Eide PK. Glymphatic MRI in idiopathic normal pressure hydrocephalus. Brain. 2017;140(10):2691-2705. doi:10.1093/ brain/awx191
- 32. Edeklev CS, Halvorsen M, Løvland G, et al. Intrathecal use of gadobutrol for glymphatic MR imaging: prospective safety study of 100 patients. Am J Neuroradiol. 2019;40(8):1257-1264. doi:10.3174/ajnr.A6136
- 33. Hovd MH, Mariussen E, Uggerud H, et al. Population pharmacokinetic modeling of CSF to blood clearance: prospective tracer study of 161 patients under work-up for CSF disorders. Fluids Barriers CNS. 2022;19(1):55. doi:10.1186/s12987-022-00352-w
- 34. Eide PK, Vinje V, Pripp AH, Mardal KA, Ringstad G. Sleep deprivation impairs molecular clearance from the human brain. Brain. 2021;144(3): 863-874. doi:10.1093/brain/awaa443
- 35. Watts R, Steinklein JM, Waldman L, Zhou X, Filippi CG. Measuring glymphatic flow in man using quantitative contrast-enhanced MRI. Am J Neuroradiol. 2019;40(4):648-651. doi:10.3174/ajnr.A5931
- 36. Dyke JP, Xu HS, Verma A, Voss HU, Chazen JL. MRI characterization of early CNS transport kinetics post intrathecal gadolinium injection: trends of subarachnoid and parenchymal distribution in healthy volunteers. Clin Imaging. 2020;68:1-6. doi:10.1016/j.clinimag.2020.04.043
- 37. Zhou Y, Cai J, Zhang W, et al. Impairment of the glymphatic pathway and putative meningeal lymphatic vessels in the aging human. Ann Neurol. 2020;87(3):357-369. doi:10.1002/ana.25670
- 38. Eide PK, Lashkarivand A, Hagen-Kersten AA, et al. Intrathecal contrast-enhanced magnetic resonance imaging of cerebrospinal fluid dynamics and glymphatic enhancement in idiopathic normal pressure hydrocephalus. Front Neurol. 2022;13:857328. doi:10.3389/fneur.2022.857328
- 39. Sperre A, Karsrud I, Rodum AHS, et al. Prospective safety study of intrathecal gadobutrol in different doses. Am J Neuroradiol. 2023;44(5):511-516. doi:10.3174/ajnr.A7841
- 40. Halvorsen M, Edeklev CS, Fraser-Green J, et al. Off-label intrathecal use of gadobutrol: safety study and comparison of administration protocols. Neuroradiology. 2021;63(1):51-61. doi:10.1007/s00234-020-02519-4
- 41. Patel M, Atyani A, Salameh JP, McInnes M, Chakraborty S. Safety of intrathecal administration of gadolinium-based contrast agents: a systematic review and meta-analysis. Radiology. 2020;297(1):75-83. doi:10.1148/radiol.2020191373
- 42. Liu S, Bilston LE, Flores Rodriguez N, et al. Changes in intrathoracic pressure, not arterial pulsations, exert the greatest effect on tracer influx in the spinal cord. Fluids Barriers CNS. 2022;19(1):14. doi:10.1186/s12987-022-00310-6
- 43. Dreha-Kulaczewski S, Joseph AA, Merboldt KD, Ludwig HC, Gärtner J, Frahm J. Inspiration is the major regulator of human CSF flow. J Neurosci. 2015;35(6):2485-2491. doi:10.1523/JNEUROSCI.3246-14.2015
- 44. Lindstrøm EK, Ringstad G, Mardal KA, Eide PK. Cerebrospinal fluid volumetric net flow rate and direction in idiopathic normal pressure hydrocephalus. Neuroimage Clin. 2018;20:731-741. doi:10.1016/j.nicl.2018.09.006
- 45. Vinje V, Zapf B, Ringstad G, Eide PK, Rognes ME, Mardal KA. Human brain solute transport quantified by glymphatic MRI-informed biophysics during sleep and sleep deprivation. Fluids Barriers CNS. 2023;20(1):62. doi:10.1186/s12987-023-00459-8
- 46. Wilson GJ, Woods M, Springer CSJ, Bastawrous S, Bhargava P, Maki JH. Human whole-blood ¹H₂O longitudinal relaxation with normal and highrelaxivity contrast reagents: influence of trans-cell-membrane water exchange. Magn Reson Med. 2014;72(6):1746-1754. doi:10.1002/mrm.25064
- 47. Hopkins AL, Yeung HN, Bratton CB. Multiple field strength in vivo T1 and T2 for cerebrospinal fluid protons. Magn Reson Med. 1986;3(2):303-311. doi:10.1002/mrm.1910030214

0991492, 2024, 9, Down

McInnis

Deutsches Zentrum Für Neurodeg,

- 48. Møllgård K, Beinlich FRM, Kusk P, et al. A mesothelium divides the subarachnoid space into functional compartments. *Science*. 2023;379(6627): 84-88. doi:10.1126/science.adc8810
- 49. Eide PK, Pripp AH, Ringstad G. Magnetic resonance imaging biomarkers of cerebrospinal fluid tracer dynamics in idiopathic normal pressure hydrocephalus. *Brain Commun.* 2020;2(2):fcaa187. doi:10.1093/braincomms/fcaa187
- 50. Taoka T, Masutani Y, Kawai H, et al. Evaluation of glymphatic system activity with the diffusion MR technique: diffusion tensor image analysis along the perivascular space (DTI-ALPS) in Alzheimer's disease cases. *Jpn J Radiol.* 2017;35(4):172-178. doi:10.1007/s11604-017-0617-z
- 51. Mestre H, Kostrikov S, Mehta RI, Nedergaard M. Perivascular spaces, glymphatic dysfunction, and small vessel disease. Clin Sci. 2017;131(17): 2257-2274. doi:10.1042/CS20160381
- 52. Eide PK, Ringstad G. Delayed clearance of cerebrospinal fluid tracer from entorhinal cortex in idiopathic normal pressure hydrocephalus: a glymphatic magnetic resonance imaging study. *J Cereb Blood Flow Metab.* 2019;39(7):1355-1368. doi:10.1177/0271678X18760974
- 53. Nedergaard M, Goldman SA. Glymphatic failure as a final common pathway to dementia. *Science*. 2020;370(6512):50-56. doi:10.1126/science.
- 54. Valnes LM, Mitusch SK, Ringstad G, Eide PK, Funke SW, Mardal KA. Apparent diffusion coefficient estimates based on 24 hours tracer movement support glymphatic transport in human cerebral cortex. *Sci Rep.* 2020;10(1):9176. doi:10.1038/s41598-020-66042-5
- 55. Melin E, Ringstad G, Valnes LM, Eide PK. Human parasagittal dura is a potential neuroimmune interface. *Commun Biol.* 2023;6(1):260. doi:10.1038/s42003-023-04634-3
- 56. Rustenhoven J, Drieu A, Mamuladze T, et al. Functional characterization of the dural sinuses as a neuroimmune interface. *Cell.* 2021;184(4): 1000-1016.e27. doi:10.1016/j.cell.2020.12.040
- 57. Ma Q, Ineichen BV, Detmar M, Proulx ST. Outflow of cerebrospinal fluid is predominantly through lymphatic vessels and is reduced in aged mice. *Nat Commun.* 2017;8(1):1434. doi:10.1038/s41467-017-01484-6
- 58. Jacob L, de Brito Neto J, Lenck S, et al. Conserved meningeal lymphatic drainage circuits in mice and humans. *J Exp Med.* 2022;219(8):e20220035. doi:10.1084/jem.20220035
- 59. Louveau A, Smirnov I, Keyes TJ, et al. Structural and functional features of central nervous system lymphatic vessels. *Nature*. 2015;523(7560): 337-341. doi:10.1038/nature14432
- 60. Ringstad G, Eide PK. Cerebrospinal fluid tracer efflux to parasagittal dura in humans. *Nat Commun.* 2020;11(1):354. doi:10.1038/s41467-019-14195-x
- 61. Shah T, Leurgans SE, Mehta RI, et al. Arachnoid granulations are lymphatic conduits that communicate with bone marrow and dura-arachnoid stroma. *J Exp Med.* 2023;220(2):e20220618. doi:10.1084/jem.20220618
- 62. Kutomi O, Takeda S. Identification of lymphatic endothelium in cranial arachnoid granulation-like dural gap. *Microscopy*. 2020;69(6):391-400. doi:10.1093/imicro/dfaa038
- 63. Ringstad G, Eide PK. Molecular trans-dural efflux to skull bone marrow in humans with CSF disorders. *Brain*. 2022;145(4):1464-1472. doi:10.1093/brain/awab388
- 64. Cugurra A, Mamuladze T, Rustenhoven J, et al. Skull and vertebral bone marrow are myeloid cell reservoirs for the meninges and CNS parenchyma. *Science*. 2021;373(6553):eabf7844. doi:10.1126/science.abf7844
- 65. Melin E, Eide PK, Ringstad G. In vivo assessment of cerebrospinal fluid efflux to nasal mucosa in humans. Sci Rep. 2020;10(1):14974. doi:10.1038/s41598-020-72031-5
- 66. Eide PK, Vatnehol SAS, Emblem KE, Ringstad G. Magnetic resonance imaging provides evidence of glymphatic drainage from human brain to cervical lymph nodes. *Sci Rep.* 2018;8(1):7194. doi:10.1038/s41598-018-25666-4
- 67. Hladky SB, Barrand MA. Mechanisms of fluid movement into, through and out of the brain: evaluation of the evidence. *Fluids Barriers CNS*. 2014; 11(1):26. doi:10.1186/2045-8118-11-26
- 68. Bakker ENTP, Naessens DMP, VanBavel E. Paravascular spaces: entry to or exit from the brain? Exp Physiol. 2019;104(7):1013-1017. doi:10.1113/EP087424
- 69. Zhao L, Tannenbaum A, Bakker ENTP, Benveniste H. Physiology of glymphatic solute transport and waste clearance from the brain. *Physiology*. 2022;37(6):349-362. doi:10.1152/physiol.00015.2022
- 70. Eide PK, Lashkarivand A, Pripp A, et al. Plasma neurodegeneration biomarker concentrations associate with glymphatic and meningeal lymphatic measures in neurological disorders. *Nat Commun.* 2023;14(1):2084. doi:10.1038/s41467-023-37685-5
- 71. Meng Y, Abrahao A, Heyn CC, et al. Glymphatics visualization after focused ultrasound-induced blood-brain barrier opening in humans. *Ann Neurol.* 2019;86(6):975-980. doi:10.1002/ana.25604
- 72. Holstein-Rønsbo S, Gan Y, Giannetto MJ, et al. Glymphatic influx and clearance are accelerated by neurovascular coupling. *Nat Neurosci.* 2023;26(6): 1042-1053. doi:10.1038/s41593-023-01327-2
- 73. Ringstad G, Valnes LM, Vatnehol SAS, Pripp AH, Eide PK. Prospective T1 mapping to assess gadolinium retention in brain after intrathecal gadobutrol. *Neuroradiology*. 2023;65(9):1321-1331. doi:10.1007/s00234-023-03198-7
- 74. Lee S, Yoo RE, Choi SH, et al. Contrast-enhanced MRI T1 mapping for quantitative evaluation of putative dynamic glymphatic activity in the human brain in sleep-wake states. *Radiology*. 2021;300(3):661-668. doi:10.1148/radiol.2021203784
- 75. Taoka T, Jost G, Frenzel T, Naganawa S, Pietsch H. Impact of the glymphatic system on the kinetic and distribution of gadodiamide in the rat brain: observations by dynamic MRI and effect of circadian rhythm on tissue gadolinium concentrations. *Invest Radiol.* 2018;53(9):529-534. doi:10.1097/RLI.0000000000000473
- 76. Mijnders LS, Steup FW, Lindhout M, van der Kleij PA, Brink WM, van der Molen AJ. Optimal sequences and sequence parameters for GBCA-enhanced MRI of the glymphatic system: a systematic literature review. *Acta Radiol.* 2021;62(10):1324-1332. doi:10.1177/0284185120969950
- 77. Naganawa S, Ito R, Kawai H, Taoka T, Yoshida T, Sone M. Confirmation of age-dependence in the leakage of contrast medium around the cortical veins into cerebrospinal fluid after intravenous administration of gadolinium-based contrast agent. *Magn Reson Med Sci.* 2020;19(4):375-381. doi:10. 2463/mrms.mp.2019-0182
- 78. Ostergaard L, Sorensen AG, Kwong KK, Weisskoff RM, Gyldensted C, Rosen BR. High resolution measurement of cerebral blood flow using intravascular tracer bolus passages. Part II: experimental comparison and preliminary results. *Magn Reson Med.* 1996;36(5):726-736. doi:10.1002/mrm. 1910360511

- 79. Ostergaard L, Weisskoff RM, Chesler DA, Gyldensted C, Rosen BR. High resolution measurement of cerebral blood flow using intravascular tracer bolus passages. Part I: mathematical approach and statistical analysis. *Magn Reson Med.* 1996;36(5):715-725. doi:10.1002/mrm.1910360510
- 80. Thrippleton MJ, Backes WH, Sourbron S, et al. Quantifying blood-brain barrier leakage in small vessel disease: review and consensus recommendations. *Alzheimers Dement*. 2019;15(6):840-858. doi:10.1016/j.jalz.2019.01.013
- 81. Reeder SB. Gadolinium-based contrast agents: What does "single-dose" mean anymore? *J Magn Reson Imaging*. 2014;39(6):1343-1345. doi:10.1002/imri 24352
- 82. Runge VM. Dechelation (transmetalation): consequences and safety concerns with the linear gadolinium-based contrast agents, in view of recent health care rulings by the EMA (Europe), FDA (United States), and PMDA (Japan). *Invest Radiol.* 2018;53(10):571-578. doi:10.1097/RLI.
- 83. Chachuat A, Molinier P, Bonnemain B, Chambon C, Gayet JL. Pharmacokinetics and tolerance of Gd-DOTA (DOTAREM) in healthy volunteers and in patients with chronic renal failure. *Eur Radiol.* 1992;2:326-329. doi:10.1007/BF00175436
- 84. van Osch MJP, Vonken EJPA, Wu O, Viergever MA, van der Grond J, Bakker CJG. Model of the human vasculature for studying the influence of contrast injection speed on cerebral perfusion MRI. *Magn Reson Med.* 2003;50(3):614-622. doi:10.1002/mrm.10567
- 85. Parker GJM, Roberts C, Macdonald A, et al. Experimentally-derived functional form for a population-averaged high-temporal-resolution arterial input function for dynamic contrast-enhanced MRI. *Magn Reson Med.* 2006;56(5):993-1000. doi:10.1002/mrm.21066
- 86. Montagne A, Barnes SR, Sweeney MD, et al. Blood-brain barrier breakdown in the aging human hippocampus. *Neuron.* 2015;85(2):296-302. doi:10. 1016/i.neuron.2014.12.032
- 87. Starr JM, Wardlaw J, Ferguson K, MacLullich A, Deary IJ, Marshall I. Increased blood-brain barrier permeability in type II diabetes demonstrated by gadolinium magnetic resonance imaging. *J Neurol Neurosurg Psychiatry*. 2003;74(1):70-76. doi:10.1136/jnnp.74.1.70
- 88. Starr JM, Farrall AJ, Armitage P, McGurn B, Wardlaw J. Blood-brain barrier permeability in Alzheimer's disease: a case-control MRI study. *Psychiatry Res.* 2009;171(3):232-241. doi:10.1016/j.pscychresns.2008.04.003
- 89. van de Haar HJ, Burgmans S, Jansen JFA, et al. Blood-brain barrier leakage in patients with early Alzheimer disease. *Radiology*. 2016;281(2):527-535. doi:10.1148/radiol.2016152244
- 90. Taheri S, Gasparovic C, Huisa BN, et al. Blood-brain barrier permeability abnormalities in vascular cognitive impairment. Stroke. 2011;42(8): 2158-2163. doi:10.1161/STROKEAHA.110.611731
- 91. Raja R, Rosenberg GA, Caprihan A. MRI measurements of blood-brain barrier function in dementia: a review of recent studies. *Neuropharmacology*. 2018;134(Pt B):259-271. doi:10.1016/j.neuropharm.2017.10.034
- 92. Manning C, Stringer M, Dickie B, et al. Sources of systematic error in DCE-MRI estimation of low-level blood-brain barrier leakage. *Magn Reson Med.* 2021;86(4):1888-1903. doi:10.1002/mrm.28833
- 93. Eide PK, Hansson HA. Blood-brain barrier leakage of blood proteins in idiopathic normal pressure hydrocephalus. *Brain Res.* 2020;1727:146547. doi: 10.1016/j.brainres.2019.146547
- 94. Wardlaw JM, Smith C, Dichgans M. Small vessel disease: mechanisms and clinical implications. *Lancet Neurol.* 2019;18(7):684-696. doi:10.1016/S1474-4422(19)30079-1
- 95. Jost G, Frenzel T, Lohrke J, Lenhard DC, Naganawa S, Pietsch H. Penetration and distribution of gadolinium-based contrast agents into the cerebrospinal fluid in healthy rats: a potential pathway of entry into the brain tissue. *Eur Radiol*. 2017;27(7):2877-2885. doi:10.1007/s00330-016-4654-2
- 96. Deike-Hofmann K, von Lampe P, Schlemmer HP, et al. The anterior eye chamber: entry of the natural excretion pathway of gadolinium contrast agents? *Eur Radiol*. 2020;30(8):4633-4640. doi:10.1007/s00330-020-06762-4
- 97. Naganawa S, Ito R, Kawamura M, Taoka T, Yoshida T, Sone M. Peripheral retinal leakage after intravenous administration of a gadolinium-based contrast agent: age dependence, temporal and inferior predominance and potential implications for eye homeostasis. *Magn Reson Med Sci.* 2023;22(1): 45-55. doi:10.2463/mrms.mp.2021-0100
- 98. Naganawa S, Suzuki K, Yamazaki M, Sakurai Y. Serial scans in healthy volunteers following intravenous administration of gadoteridol: time course of contrast enhancement in various cranial fluid spaces. *Magn Reson Med Sci.* 2014;13(1):7-13. doi:10.2463/mrms.2013-0056
- 99. Wåhlin A, Garpebring A, Mogensen K, et al. Quantitative imaging of brain to cerebrospinal fluid molecular clearance. In: *Proceedings of the International Society for Magnetic Resonance in Medicine*. London; 2022;327.
- 100. Cao D, Kang N, Pillai JJ, et al. Fast whole brain MR imaging of dynamic susceptibility contrast changes in the cerebrospinal fluid (cDSC MRI). *Magn Reson Med.* 2020;84(6):3256-3270. doi:10.1002/mrm.28389
- 101. Antony J, Hacking C, Jeffree RL. Pachymeningeal enhancement-a comprehensive review of literature. *Neurosurg Rev.* 2015;38(4):649-659. doi:10. 1007/s10143-015-0646-y
- 102. Balin BJ, Broadwell RD, Salcman M, El-Kalliny M. Avenues for entry of peripherally administered protein to the central nervous system in mouse, rat, and squirrel monkey. *J Comp Neurol.* 1986;251(2):260-280. doi:10.1002/cne.902510209
- 103. ladecola C, Smith EE, Anrather J, et al. The neurovasculome: key roles in brain health and cognitive impairment: a scientific statement from the American Heart Association/American Stroke Association. Stroke. 2023;54(6):e251-e271. doi:10.1161/STR.0000000000000431
- 104. Richmond SB, Rane S, Hanson MR, et al. Quantification approaches for magnetic resonance imaging following intravenous gadolinium injection: a window into brain-wide glymphatic function. *Eur J Neurosci.* 2023;57(10):1689-1704. doi:10.1111/ejn.15974
- 105. Yuan W, Lv Y, Zeng M, Fu BM. Non-invasive measurement of solute permeability in cerebral microvessels of the rat. *Microvasc Res.* 2009;77(2): 166-173. doi:10.1016/j.mvr.2008.08.004
- 106. Mayhan WG, Heistad DD. Permeability of blood-brain barrier to various sized molecules. *Am J Physiol.* 1985;248(5 Pt 2):H712-H718. doi:10.1152/ajpheart.1985.248.5.H712
- 107. Absinta M, Ha SK, Nair G, et al. Human and nonhuman primate meninges harbor lymphatic vessels that can be visualized noninvasively by MRI. *Elife*. 2017;6:6. doi:10.7554/eLife.29738
- 108. Freeze WM, Schnerr RS, Palm WM, et al. Pericortical enhancement on delayed postgadolinium fluid-attenuated inversion recovery images in normal aging, mild cognitive impairment, and Alzheimer disease. *Am J Neuroradiol.* 2017;38(9):1742-1747. doi:10.3174/ajnr.A5273
- 109. Naganawa S, Nakane T, Kawai H, Taoka T. Gd-based contrast enhancement of the perivascular spaces in the basal ganglia. *Magn Reson Med Sci.* 2017;16(1):61-65. doi:10.2463/mrms.mp.2016-0039

0991492, 2024, 9, Down

McInnis -

Deutsches Zentrum F
ür Neurodeg, Wiley Online Library on [08/08/2024]. See the

- 110. Hansen TP, Cain J, Thomas O, Jackson A. Dilated perivascular spaces in the basal ganglia are a biomarker of small-vessel disease in a very elderly population with dementia. *Am J Neuroradiol.* 2015;36(5):893-898. doi:10.3174/ajnr.A4237
- 111. Bouvy WH, Biessels GJ, Kuijf HJ, Kappelle LJ, Luijten PR, Zwanenburg JJM. Visualization of perivascular spaces and perforating arteries with 7 T magnetic resonance imaging. *Invest Radiol.* 2014;49(5):307-313. doi:10.1097/RLI.0000000000000027
- 112. Naganawa S, Nakane T, Kawai H, Taoka T. Differences in signal intensity and enhancement on MR images of the perivascular spaces in the basal ganglia versus those in white matter. Magn Reson Med Sci. 2018;17(4):301-307. doi:10.2463/mrms.mp.2017-0137
- 113. Groeschel S, Chong WK, Surtees R, Hanefeld F. Virchow-Robin spaces on magnetic resonance images: normative data, their dilatation, and a review of the literature. *Neuroradiology*. 2006;48(10):745-754. doi:10.1007/s00234-006-0112-1
- 114. Wardlaw JM, Benveniste H, Nedergaard M, et al. Perivascular spaces in the brain: anatomy, physiology and pathology. *Nat Rev Neurol.* 2020;16(3): 137-153. doi:10.1038/s41582-020-0312-z
- 115. Naganawa S, Nakane T, Kawai H, Taoka T. Lack of contrast enhancement in a giant perivascular space of the basal ganglion on delayed FLAIR images: implications for the glymphatic system. *Magn Reson Med Sci.* 2017;16(2):89-90. doi:10.2463/mrms.ci.2016-0114
- 116. Wang X, Lou N, Eberhardt A, et al. An ocular glymphatic clearance system removes β-amyloid from the rodent eye. *Sci Transl Med.* 2020;12(536): eaaw3210. doi:10.1126/scitranslmed.aaw3210
- 117. Deike-Hofmann K, von Lampe P, Eerikaeinen M, et al. Anterior chamber enhancement predicts optic nerve infiltration in retinoblastoma. *Eur Radiol.* 2022;32(11):7354-7364. doi:10.1007/s00330-022-08778-4
- 118. Taoka T, Naganawa S. Gadolinium-based contrast media, cerebrospinal fluid and the glymphatic system: possible mechanisms for the deposition of gadolinium in the brain. *Magn Reson Med Sci.* 2018;17(2):111-119. doi:10.2463/mrms.rev.2017-0116
- 119. Galluzzi P, Cerase A, Hadjistilianou T, et al. Retinoblastoma: abnormal gadolinium enhancement of anterior segment of eyes at MR imaging with clinical and histopathologic correlation. *Radiology*. 2003;228(3):683-690. doi:10.1148/radiol.2283020466
- 120. Manava P, Eckrich C, Luciani F, Schmidbauer J, Lell MM, Detmar K. Glymphatic system in ocular diseases: evaluation of MRI findings. Am J Neuroradiol. 2022;43(7):1012-1017. doi:10.3174/ajnr.A7552
- 121. Mehta NH, Sherbansky J, Kamer AR, et al. The brain-nose interface: a potential cerebrospinal fluid clearance site in humans. *Front Physiol.* 2021;12: 769948. doi:10.3389/fphys.2021.769948
- 122. Norwood JN, Zhang Q, Card D, Craine A, Ryan TM, Drew PJ. Anatomical basis and physiological role of cerebrospinal fluid transport through the murine cribriform plate. Elife. 2019;8:8. doi:10.7554/eLife.44278
- 123. Stanton EH, Persson NDÅ, Gomolka RS, et al. Mapping of CSF transport using high spatiotemporal resolution dynamic contrast-enhanced MRI in mice: effect of anesthesia. *Magn Reson Med.* 2021;85(6):3326-3342. doi:10.1002/mrm.28645
- 124. Boulton M, Flessner M, Armstrong D, Hay J, Johnston M. Lymphatic drainage of the CNS: effects of lymphatic diversion/ligation on CSF protein transport to plasma. Am J Physiol. 1997;272(5 Pt 2):R1613-R1619. doi:10.1152/ajpregu.1997.272.5.R1613
- 125. Boulton M, Flessner M, Armstrong D, Mohamed R, Hay J, Johnston M. Contribution of extracranial lymphatics and arachnoid villi to the clearance of a CSF tracer in the rat. Am J Physiol. 1999;276(3):R818-R823. doi:10.1152/ajpregu.1999.276.3.R818
- 126. Bradbury MW, Cserr HF, Westrop RJ. Drainage of cerebral interstitial fluid into deep cervical lymph of the rabbit. *Am J Physiol.* 1981;240(4):F329-F336. doi:10.1152/ajprenal.1981.240.4.F329
- 127. Sennfält S, Thrippleton MJ, Stringer M, et al. Visualising and semi-quantitatively measuring brain fluid pathways, including meningeal lymphatics, in humans using widely available MRI techniques. *J Cereb Blood Flow Metab*. 2023;43(10):1779-1795. doi:10.1177/0271678X231179555
- 128. Naganawa S, Ito R, Kato Y, et al. Intracranial distribution of intravenously administered gadolinium-based contrast agent over a period of 24 hours: evaluation with 3D-real IR imaging and MR fingerprinting. *Magn Reson Med Sci.* 2021;20(1):91-98. doi:10.2463/mrms.mp.2020-0030
- 129. Varatharaj A, Carare RO, Weller RO, Gawne-Cain M, Galea I. Gadolinium enhancement of cranial nerves: implications for interstitial fluid drainage from brainstem into cranial nerves in humans. *Proc Natl Acad Sci U S A.* 2021;118(45):e2106331118. doi:10.1073/pnas.2106331118
- 130. Naganawa S, Taoka T, Kawai H, Yamazaki M, Suzuki K. Appearance of the organum vasculosum of the lamina terminalis on contrast-enhanced MR imaging. *Magn Reson Med Sci.* 2018;17(2):132-137. doi:10.2463/mrms.mp.2017-0088
- 131. Bèchet NB, Shanbhag NC, Lundgaard I. Glymphatic pathways in the gyrencephalic brain. *J Cereb Blood Flow Metab*. 2021;41(9):2264-2279. doi:10. 1177/0271678X21996175
- 132. Mestre H, Tithof J, Du T, et al. Flow of cerebrospinal fluid is driven by arterial pulsations and is reduced in hypertension. *Nat Commun.* 2018;9(1): 4878. doi:10.1038/s41467-018-07318-3
- 133. Kiviniemi V, Wang X, Korhonen V, et al. Ultra-fast magnetic resonance encephalography of physiological brain activity—glymphatic pulsation mechanisms? *J Cereb Blood Flow Metab*. 2016;36(6):1033-1045. doi:10.1177/0271678X15622047
- 134. Benveniste H, Liu X, Koundal S, Sanggaard S, Lee H, Wardlaw J. The glymphatic system and waste clearance with brain aging: a review. *Gerontology*. 2019;65(2):106-119. doi:10.1159/000490349
- 135. Pardridge WM. CSF, blood-brain barrier, and brain drug delivery. *Expert Opin Drug Deliv.* 2016;13(7):963-975. doi:10.1517/17425247.2016. 1171315
- 136. Gergelé L, Manet R. Postural regulation of intracranial pressure: a critical review of the literature. *Acta Neurochir Suppl.* 2021;131:339-342. doi:10. 1007/978-3-030-59436-7_65
- 137. Eftekhari S, Westgate CSJ, Johansen KP, Bruun SR, Jensen RH. Long-term monitoring of intracranial pressure in freely-moving rats; impact of different physiological states. Fluids Barriers CNS. 2020;17(1):39. doi:10.1186/s12987-020-00199-z
- 138. de Leon MJ, Li Y, Okamura N, et al. Cerebrospinal fluid clearance in Alzheimer disease measured with dynamic PET. *J Nucl Med.* 2017;58(9): 1471-1476. doi:10.2967/jnumed.116.187211
- 139. Mestre H, Mori Y, Nedergaard M. The brain's glymphatic system: current controversies. *Trends Neurosci.* 2020;43(7):458-466. doi:10.1016/j.tins. 2020.04.003
- 140. Iliff JJ, Lee H, Yu M, et al. Brain-wide pathway for waste clearance captured by contrast-enhanced MRI. J Clin Invest. 2013;123(3):1299-1309. doi: 10.1172/JCI67677
- 141. Lassen NA, Perl W. Tracer Kinetic Methods in Medical Physiology. Raven Press; 1979.
- 142. Raghunandan A, Ladron-de-Guevara A, Tithof J, et al. Bulk flow of cerebrospinal fluid observed in periarterial spaces is not an artifact of injection. *Elife.* 2021;10:10. doi:10.7554/eLife.65958

- 143. van Veluw SJ, Hou SS, Calvo-Rodriguez M, et al. Vasomotion as a driving force for paravascular clearance in the awake mouse brain. *Neuron.* 2020; 105(3):549-561.e5. doi:10.1016/j.neuron.2019.10.033
- 144. Kameda H, Kinota N, Kato D, et al. Magnetic resonance water tracer imaging using 17 O-labeled water. *Invest Radiol.* 2024;59(1):92-103. doi:10. 1097/RLI.000000000001021
- 145. Kudo K, Harada T, Kameda H, et al. Indirect MRI of (17) o-labeled water using steady-state sequences: signal simulation and preclinical experiment. *J Magn Reson Imaging*. 2018;47(5):1373-1379. doi:10.1002/jmri.25848
- 146. Alshuhri MS, Gallagher L, Work LM, Holmes WM. Direct imaging of glymphatic transport using H2170 MRI. *JCI Insight*. 2021;6(10):141159. doi:10. 1172/jci.insight.141159
- 147. Helakari H, Korhonen V, Holst SC, et al. Human NREM sleep promotes brain-wide vasomotor and respiratory pulsations. *J Neurosci.* 2022;42(12): 2503-2515. doi:10.1523/JNEUROSCI.0934-21.2022
- 148. Rajna Z, Mattila H, Huotari N, et al. Cardiovascular brain impulses in Alzheimer's disease. *Brain.* 2021;144(7):2214-2226. doi:10.1093/brain/awab144

SUPPORTING INFORMATION

Additional supporting information can be found online in the Supporting Information section at the end of this article.

How to cite this article: van Osch MJP, Wåhlin A, Scheyhing P, et al. Human brain clearance imaging: Pathways taken by magnetic resonance imaging contrast agents after administration in cerebrospinal fluid and blood. *NMR in Biomedicine*. 2024;37(9):e5159. doi:10. 1002/nbm.5159